N71-28018

NASA CONTRACTOR
REPORT

NASA CR-61354

CASE FILE
COPY

FASTENER LOAD ANALYSIS METHOD

By Fred R. Rollins, Jr.

Midwest Research Institute
425 Volker Boulevard
Kansas City, Mo. 64110

April 2, 1971

Final Report

Prepared for

NASA-GEORGE C. MARSHALL SPACE FLIGHT CENTER
Marshall Space Flight Center, Alabama 35812

TECHNICAL REPORT STANDARD TITLE PAGE

1. REPORT NO.	2. GOVERNMENT ACCESSION NO.	3. RECIPIENT'S CATALOG NO.
NASA CR-61354		

4. TITLE AND SUBTITLE	5. REPORT DATE
FASTENER LOAD ANALYSIS METHOD	April 2, 1971
	6. PERFORMING ORGANIZATION CODE
7. AUTHOR(S) Fred R. Rollins, Jr.	8. PERFORMING ORGANIZATION REPORT # DCN-1-0-60-00081(1F)
9. PERFORMING ORGANIZATION NAME AND ADDRESS Midwest Research Institute 425 Volker Boulevard Kansas City, Mo. 64110	10. WORK UNIT NO.
	11. CONTRACT OR GRANT NO. NAS 8-25362
12. SPONSORING AGENCY NAME AND ADDRESS National Aeronautics and Space Administration Washington, D. C. 20546	13. TYPE OF REPORT & PERIOD COVERED Final Contractor Report 28 January 1970 - Apr. 1971
	14. SPONSORING AGENCY CODE

15. SUPPLEMENTARY NOTES

16. ABSTRACT

This report covers an investigation into the feasibility of analyzing bolt preloads by ultrasonic techniques. Various techniques were evaluated and a pulse echo interferometric method was selected for experimental testing. In agreement with theoretical predictions, the interferometer response was found to be linearly related to tensile stresses oriented parallel to the bolt axis. Under rather idealized conditions, bolt loads can be determined with errors of less than 1%. The ultimate operational accuracy depends on a number of variables, such as bolt dimensions and geometry, bolt temperature, uniformity of stresses, and bolt materials, but load analyses to within ± 3% are readily achievable. Best results are obtained with the ultrasonic transducer contact coupled to a small flat area near the center of the bolt head. The transducer can be applied and measurements made without interfering with normal wrenching operations. Prototype instrumentation is described and calibration results are tabulated for numerous bolt sizes and materials. The possibility of using this instrumentation for rechecking bolt loads subsequent to assembly is also discussed.

17. KEY WORDS	18. DISTRIBUTION STATEMENT
Ultrasonic Pulse echo interferometric method	Unclassified - unlimited George W. Kurtz

19. SECURITY CLASSIF. (of this report)	20. SECURITY CLASSIF. (of this page)	21. NO. OF PAGES	22. PRICE
Unclassified	Unclassified	66	$3.00

MSFC - Form 3292 (May 1969)

PREFACE

This report was prepared for the George C. Marshall Space Flight Center of the National Aeronautics and Space Administration under Contract No. NAS8-25362. The program was monitored by Mr. George Kurtz of the Marshall Space Flight Center.

The program activity covered by this report was performed during the period 28 January 1970 to 1 April 1971. The objective of the program was to evaluate the feasibility of using ultrasonic techniques as a tool for the accurate analysis of bolt loads, primarily during tightening or assembly operations. The actual work involved selection and development of a suitable technique plus a variety of tests and experiments designed to evaluate reproducibility and sources of error. The results are quite encouraging and indicate that ultrasonic techniques can be used to set fastener preloads. The technique has a potential accuracy considerably higher than that attainable with torque wrenches or PLI-washers. A prototype instrument was assembled and calibration data collected for numerous bolts.

The subject project was conducted by Midwest Research Institute under the administrative supervision of Dr. H. M. Hubbard, Director of the Physical Sciences Division, and Mr. G. E. Gross, Head of the Materials Science Section. Mr. F. R. Rollins, Jr., served as project leader. Mr. Gerald Swanson provided valuable assistance in both program planning and experimental execution.

Approved for:

MIDWEST RESEARCH INSTITUTE

H. M. Hubbard, Director
Physical Sciences Division

2 April 1971

pl

TABLE OF CONTENTS

		Page No.
I.	Introduction	1
II.	Requirements and Technique Selection	2
III.	The Frequency-Null Technique	4
IV.	Factors Affecting Accuracy	10
	A. Transducer Coupling	16
	B. Bolt-End Geometry and Surface Condition	17
	C. Length	18
	D. Temperature	21
	E. Plastic Yielding	21
	F. Shear Stresses	25
	G. Bending	27
V.	NASA Supplied Bolts (Phase I)	29
VI.	Prototype Instrumentation	31
VII.	Calibration Results	45
VIII.	Recheck Capability	54
IX.	Conclusions and Recommendations	55
References		58
Appendix A		59

List of Tables

Table No.	Title	Page No.
I	Information on NASA Bolts Investigated During Phase I	13
II	Summary of Calibration Data	50

TABLE OF CONTENTS (Continued)

List of Figures

Figure No.	Title	Page No.
1	Sketches of Bolts Showing Effect of Stress.	3
2	Block Diagram of Frequency-Null Interferometer.	5
3	Oscillograms Showing Pulse-Echo Pattern (Top), Same Pattern After Mixture of CW Signal (Center), and Expanded Sweep Presentation of Mixed Signal with Frequency Adjusted for Null Condition at First Echo .	7
4	Bolt and Nut Diagrams Showing Relationships Between Total Length, ℓ_t , and Stressed Lengths, ℓ_s and $\ell_{s'}$, for Totally Threaded Bolts (1a) and Partially Threaded Bolts (1b)	9
5	NASA Supplied Bolts	11
6	Bolts Purchased Locally for Frequency-Null Inspection .	12
7	MRI-1 Aluminum Bolt With Transducer Held in Place With Yoke Arrangement.	14
8	Frequency Change Vs. Bolt Load for Three MRI Bolts. . .	15
9	Response Curves for an Aluminum Bolt With Indicated Stressed Length	19
10	Response Curves for Two Aluminum Bolts of the Same Stressed Length but With Different Real Length as Indicated	20
11	Changes in Null Frequency Versus Temperature for Two NASA Supplied Bolts	22
12	Frequency Change Versus Load for an (MRI-1) Aluminum Bolt Held at the Indicated Temperatures During the Loading Operation	23
13	Loading and Unloading Curves for an Aluminum Bolt Stressed Beyond the Yield Strength.	24

TABLE OF CONTENTS (Continued)

List of Figures (Continued)

Figure No.	Title	Page No.
14	Frequency Change Versus Load for Three Identical 3/4-In. Aluminum Bolts Loaded in (A) Pure Tension, (B) Torque-Tension With Threads Lubricated, and (C) Torque-Tension Without Lubrication.	26
15	Frequency-Versus-Load Curves for an Aluminum Bolt With (A) 0 Mils, (B) 10 Mils, (C) 20 Mils, and (D) 30 Mils of Steel Shimstock Under One Side of the Bolt Head to Induce Bending During the Loading Operation	28
16	Frequency Change Versus Load for Four NASA Supplied Bolts	30
17	Frequency Change Versus Load for Several Different Bolt Sizes and Alloys.	32
18	Normalized Frequency Change Versus Stress for NASA Supplied Bolts.	33
19	Frequency Change Versus Stress for 3/8-In. and 3/4-In. Bolts of 4140 Steel	34
20	Photograph of Prototype Instrumentation Being Used to Set Bolt Preloads on a Vacuum System.	35
21	Block Diagram of Prototype Fastener Load Analyzer . . .	36
22	Oscillograms Showing Scope Presentation From (a) a 3/4-In. 431 Stainless Steel Bolt (AN 12C-36A), and (b) a 5/16-In. Aluminum Bolt (AN5 DD-11A)	38
23	Oscillograms From a 5/16-In. Aluminum Bolt (AN5 DD-11A) With the Phase Detected Signal (Top Trace) of the First Echo Centered in the Horizontal Direction . . .	39
24	Oscillograms From a 3/4-In. Stainless Steel Bolt (AN 12C-36A) With the Phase Detected Signal (Top Trace) of the First Echo Centered in the Horizontal Direction	40

TABLE OF CONTENTS (Concluded)

List of Figures (Concluded)

Figure No.	Title	Page No.
25	Prototype Socket Wrench With Spring Loaded Transducer (Top) and Modified Socket Wrench With Electrical Contact for Separate Transducer (Bottom).	42
26	Cross-Sectional View of Small Cylindrical Transducer Unit Mounted on Bolt Head	44
27	Several Transducer Housings Designed for Specific Bolt Applications	46
28	Examples of Transducers and Wrench Connectors for Two Different Bolt Head Configurations.	47
29	Additional Bolts for Which Calibration Data Were Collected	48
30	Δf-Versus-Load for Two Different 3/4-In. Bolts of 431 Stainless Steel	52

I. INTRODUCTION

It has been known for some time that stresses in metals and other solids can produce small changes in the velocity of propagation of ultrasonic waves.[1,2] These stress-induced velocity effects are relatively small when compared to velocity changes due to other variables, such as alloy differences or preferred grain orientation. Because the stress effect is relatively weak it has not found widespread use in stress analysis applications even though considerable research has been directed toward this end, particularly in regard to the analysis of residual stresses. This program was initiated to determine the feasibility of using stress-induced changes in ultrasonic propagation parameters in analyzing the preload on aerospace fasteners, particularly threaded bolts.

There are two distinctly different applications for an ultrasonic load analyzer. The first application involves the analysis of load or stress levels during actual assembly, i.e., while the bolt is being tightened. In this application we might think of the ultrasonic measurement as a substitute for torque wrench readings. Since ultrasonic techniques will probably be more complicated, they must have significant advantages, such as improved accuracy, if they are to be used over the torque wrench which often exhibits errors of ± 25%. The original goal of this program, as set by NASA, was to develop a technique which would permit bolt preloads to be established with errors of only ± 1%.

The second potential application of ultrasound to bolt load analysis is in evaluating the post-assembly load, perhaps weeks or months after assembly and possibly after exposure to various environments including intense vibration. In this application, the torque wrench is of little value unless the bolts can be loosened and retorqued. At the present time there is no satisfactory answer to the post-assembly load analysis problem.

The two analysis problems discussed above also place very different requirements on an ultrasonic system. In this program, major emphasis has been placed on load analysis during assembly, but the post-assembly problem has been investigated also.

This report contains a discussion of fastener load measurement problems together with a rather complete description of the tests and analyses performed during this program. As expected, the ultrasonic results are very dependent on the geometry and surface condition of both the head and threaded end of a given bolt configuration. Under rather idealized conditions, ultrasonic measurements can be related to bolt loads with errors of less than ± 1%. The errors generally increase as the idealized conditions degenerate, but during the course of this program it has been demonstrated

that in simulated torquing operations on some "as received" bolts, the ultrasonic technique can yield reproducible results with errors of about 3%. Factors which may produce larger errors have been investigated and the results are discussed in this report.

II. REQUIREMENTS AND TECHNIQUE SELECTION

As mentioned in the introduction, the velocity of ultrasonic waves in a metal is influenced slightly by stress. Some techniques, based on ultrasonic shear waves,[3] can be used to evaluate stress-induced velocity changes without any additional influence from the dimensional changes which normally accompany the stress. However, such techniques are not readily applicable to bolts because the stress direction must be perpendicular to the propagation direction. In the bolt load problem, these two directions are collinear. It is also difficult to separate velocity and length effects so we necessarily evaluate the combined effect of both length and velocity.

In order to better understand the velocity and length changes produced by a tensile load, consider the bolt sketches shown in Figure 1. The bolt is stretched in normal applications where the tensile stress within the bolt counteracts some external force. The overall length increases by some increment $\Delta \ell$ and the velocity in the stressed region may change by an increment Δv, which we will assume can be either positive or negative. Although we are primarily interested in the stressed region, we are forced to examine ultrasonic parameters which are also influenced by metal outside of the stressed region. For example, assume that the round trip transit time of an ultrasonic pulse is to be evaluated as the pulse travels from the bolt head to the threaded end and back to the head. The transit time in the stressed bolt is dependent on both $\Delta \ell$ and Δv. We can assume that $\frac{\Delta \ell}{\ell}$ is less than the strain produced by yield point stresses, i.e., approximately 0.2%. Previous measurements[2] suggest that $\frac{\Delta v}{v}$ is of the same order of magnitude. Thus, the fractional change in transit time, $\frac{\Delta T}{T}$ can be estimated to be in the range 10^{-2} to 10^{-3}. Adequate measurement of such small changes normally requires techniques with errors of less than 1 part in 10^4 to 10^5, considerably beyond standard pulse-echo transit time measurements. Some form of ultrasonic interferometry is usually necessary for such accuracies.

During the early phases of this program, preliminary experiments were performed to confirm the magnitude of the expected effect and to demonstrate that interferometric techniques could be applied to the problem. A literature search was made to uncover all potential techniques, of which

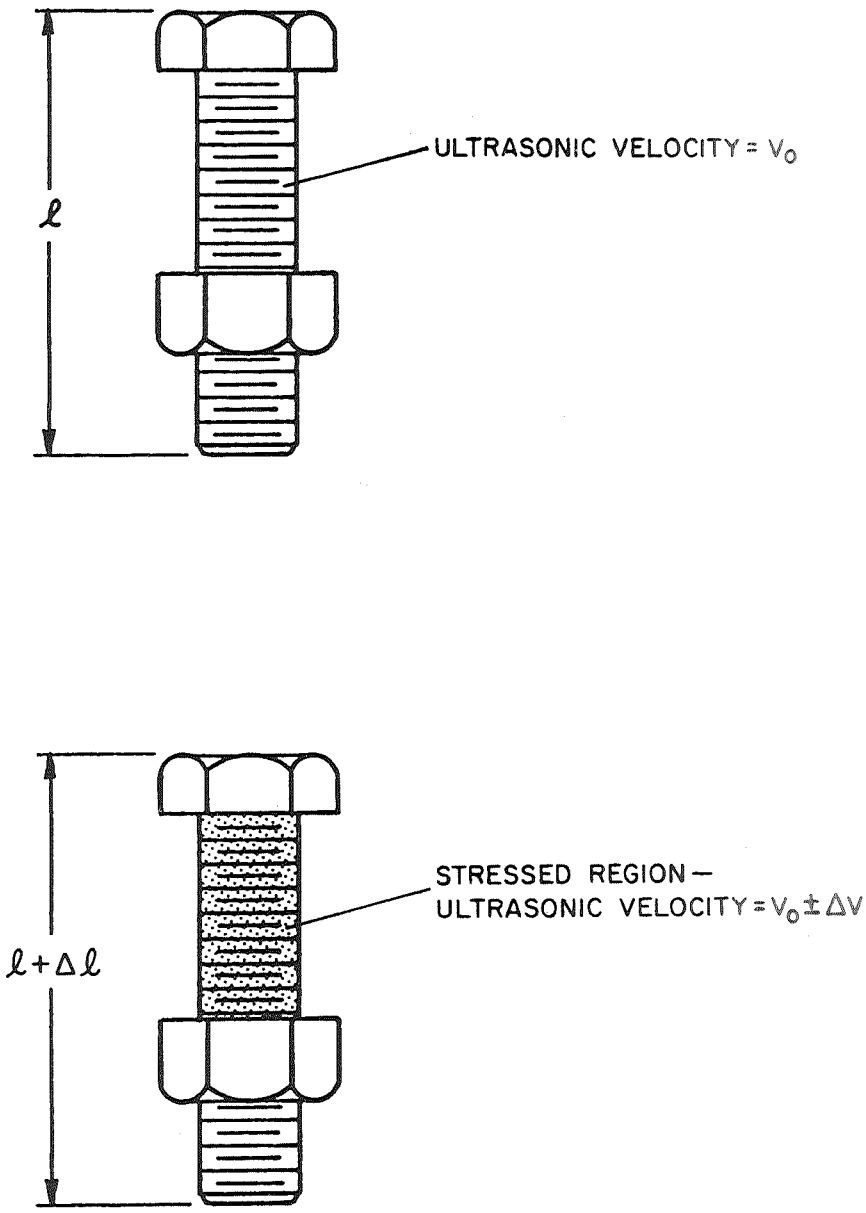

Figure 1 - Sketches of Bolts Showing Effect of Stress

the most promising were selected for further study and experimentation. The techniques which received primary study included the two-specimen interferometer,[4] pulse superposition,[5] pulse-echo overlap,[6] and an interferometric method first described by Pervushin and Filippov,[7] but subsequently modified by Benson and Associates[8] and called the frequency-null technique. All of these techniques theoretically have sufficient accuracy for the bolt load analysis problem so final selection was primarily based on relative simplicity and applicability to ultimate field type testing. The two-specimen interferometer does not yield continuous readings as readily as the frequency-null technique; furthermore, it requires a relatively large number of echoes whereas the frequency-null technique requires only one echo. Multiple echoes (at least two) are also required for both the pulse superposition and pulse-echo overlap technique. There are several advantages in using only the first echo. Generally the first echo is the strongest (in fact, it may be the only one available) and is less complicated by interference with unwanted noise. Thus, a modified frequency-null technique was selected for major experimental testing and is described in Section III.

During the later months of this program we became aware of some research by other workers concerned with the ultrasonic measurement of bolt loads. H. J. McFaul and co-workers[9] have developed a compact instrument which essentially measures the change in ultrasonic round trip transit time as the bolt is loaded. Readout is accomplished with a meter, the scale of which is marked in units of elongation. The referenced report[9] does not include enough data to really establish performance characteristics, but we are confident that the inherent accuracy of the time-of-flight measurement is considerably less than the interferometer method used in this program. Nevertheless, the greater compactness and ease of operation of the time-of-flight instrument are important advantages. The desired accuracy will ultimately govern the preferred instrumentation.

III. THE FREQUENCY-NULL TECHNIQUE

A simplified diagram of instrumentation for the frequency-null technique is shown in Figure 2. The signal generator provides a variable frequency CW signal which is fed to a frequency counter and a gated amplifier. The gated rf pulse from the amplifier drives the piezoelectric transducer which is coupled to one end of the bolt under investigation. Using this arrangement, the frequency of the rf pulse is controlled at the signal generator and can be accurately determined by the frequency counter. The electrical signals created at the transducer by ultrasonic echoes from the opposite end of the bolt are then fed through a TR switch to one input of a differential preamplifier on the oscilloscope. The TR switch is utilized

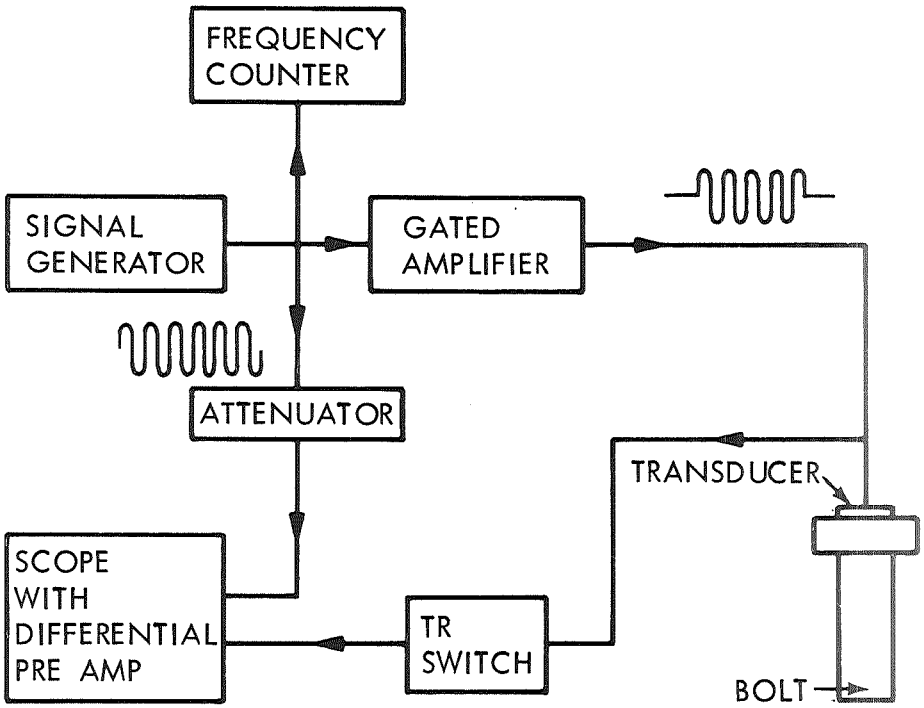

Figure 2 - Block Diagram of Frequency-Null Interferometer

to reduce saturation in the preamplifier by blocking passage of the large driving pulse and permitting the weaker echoes to pass. Part of the CW signal from the signal generator serves as the other input to the differential preamplifier where it is ultimately mixed with the echo signals from the bolt.

Any of the pulse echoes can be utilized in taking data but we have emphasized use of the first echo because it is less likely to be confused by unwanted signals from side wall reflections, beam spreading, slower modes, etc. Data are obtained by varying the frequency and amplitude of the first echo until almost complete destructive interference between the CW and pulse signal is observed on the oscilloscope. The frequency as determined by the counter is then recorded. If a stress is applied to the bolt, the frequency must be varied in order to maintain the interference, or null condition.

Oscillograms showing various echo patterns and frequency-null presentations are shown in Figure 3. The top oscillogram is simply the pulse-echo pattern from an aluminum bolt. The center photo shows the same pattern after mixing with the CW signal. The bottom photo shows the mixed pattern at an expanded sweep and with the frequency adjusted for null conditions at the first echo. Clean echoes such as those shown in Figure 3 can be reproducibly nulled with frequency variations of less than 100 Hz. Assuming a typical CW frequency of 10 MHZ it is clear that a given null frequency can be determined with an error of about 1 part in 10^5.

In the prototype instrumentation, developed in this program and described in more detail later, a phase detector circuit was added to the diagram of Figure 2. The output of the phase detector, as displayed on the scope and used to monitor the null condition, is less sensitive to amplitude variations and thus facilitates operation.

As mentioned previously, the frequency required to maintain a given null condition varies with the stress or load on the bolt. Appendix A includes a simple derivation for the interdependence between the null frequency and the stress or load condition. For bolts which are threaded over the full length (see Figure 4a), the expression relating the fractional change in frequency, $\frac{\Delta f}{f}$, and the stress, S, or load, L, is as follows:

$$\frac{\Delta f}{f} \cong \frac{\ell_s}{\ell_t} (\beta/2 - \alpha) S, \text{ or } \frac{\Delta f}{f} \cong \frac{\ell_s}{\ell_t} (\beta/2 - \alpha) \frac{L}{A_s} \qquad (1)$$

where ℓ_t is the total length of the bolt, ℓ_s is the length subjected to stress (defined approximately as the distance between the head and nut as shown in Figure 4a), and A_s is the effective cross sectional area of the threads.

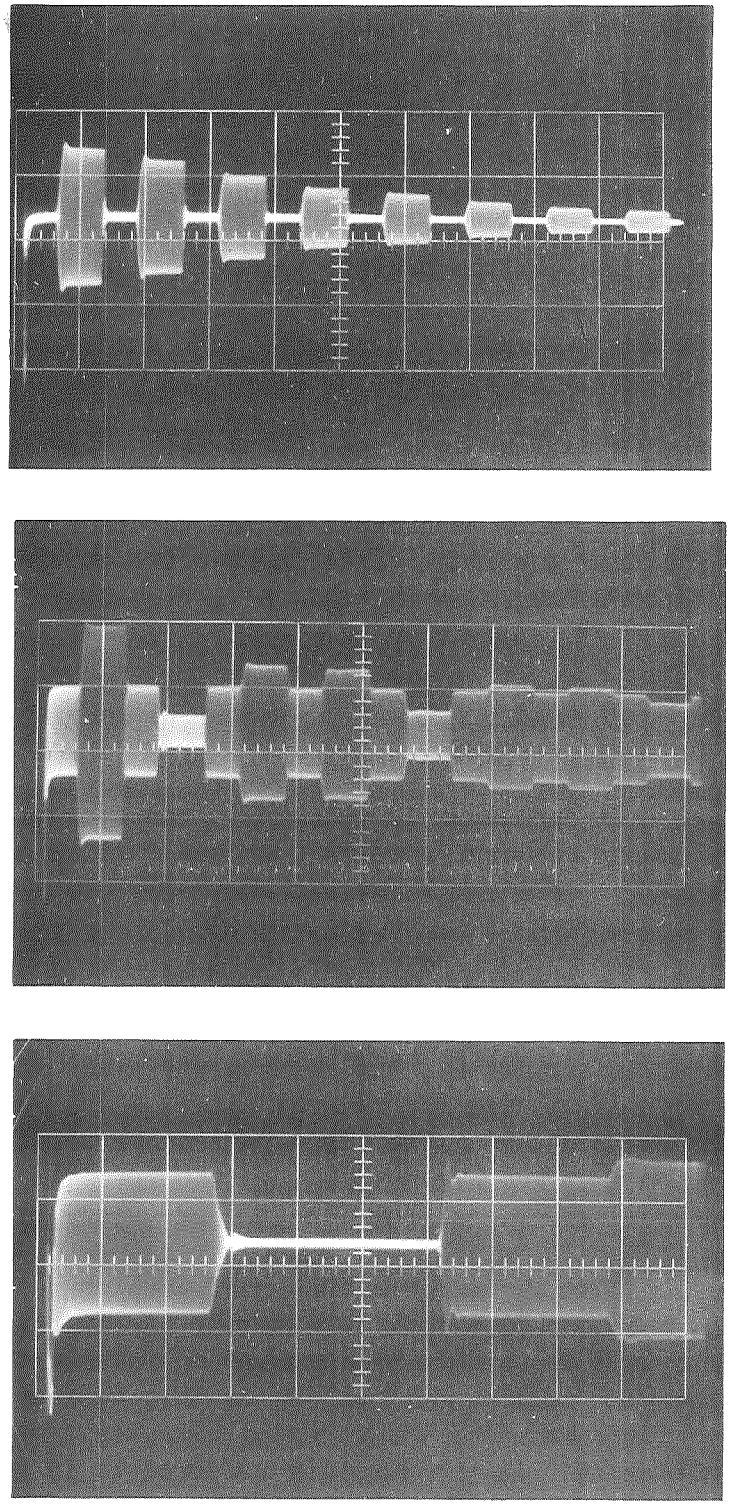

Figure 3 - Oscillograms Showing Pulse Echo Pattern (Top), Same Pattern After Mixture With CW Signal (Center), and Expanded Sweep Presentation of Mixed Signal With Frequency Adjusted for Null Condition at First Echo

The term, $(\beta/2 - \alpha)$, is a constant for a given material but differs from one metal to another. Beta is a complex term containing material constants which define the stress-induced change in velocity, whereas α is simply the reciprocal of Young's modulus and defines the stress-induced change in length. Expression (1) is strictly valid only for stresses below the yield strength. Thus, in the elastic region Δf should be linearly related to stress.

Expression (1) is also based on a uniform stress over the length ℓ_s. However, in a partially threaded bolt, such as that shown in Figure 4b, it is clear that ℓ_s is divided into two distinct stress areas. Since the effective diameter of the threaded area is less than that of the unthreaded area, the stress will be greater in the threaded portion. It is a simple task to modify Expression (1) to include two stressed lengths, ℓ_s and $\ell_{s'}$, subject to stresses S and S', respectively. The result is

$$\frac{\Delta f}{f} \simeq \frac{(\beta/2 - \alpha)}{\ell_t} (S\,\ell_s + S'\,\ell_{s'}) \qquad (2)$$

Since the stress in each sublength is related to the overall load, L, and the effective cross-sectional area A, we can further modify (2) as follows:

$$\frac{\Delta f}{f} \simeq \frac{(\beta/2 - \alpha)}{\ell_t} \left(\frac{\ell_s}{A_s} + \frac{\ell_{s'}}{A_{s'}}\right) L \qquad (3)$$

Thus $\Delta f/f$ is still linear in L, but for a given alloy and load, we see that $\Delta f/f$ also depends on five dimensions, all of which must be considered in determining the desired Δf value for a particular bolt application.

It should be emphasized that when the frequency is varied over a wide range many null conditions are observed. From Appendix A one can see that nulls occur each time an integral number of wavelengths fit into the bolt length. When the load on a bolt is altered, during tightening for example, we attempt to maintain the same number of wavelengths within the bolt by keeping the same null condition. To do this we must alter the frequency, f, to compensate for the changing ultrasonic velocity and bolt length. The resulting Δf is the quantity referred to in Expressions (1)-(3).

Another frequency difference, ΔF, which can be measured using the frequency-null technique is obtained by evaluating the frequencies of adjacent nulls, i.e., two interference conditions represented by n and $(n+1)$ wavelengths within the specimen. The value of ΔF is related to the total transit time, T, as follows: $\Delta F = 1/T$.

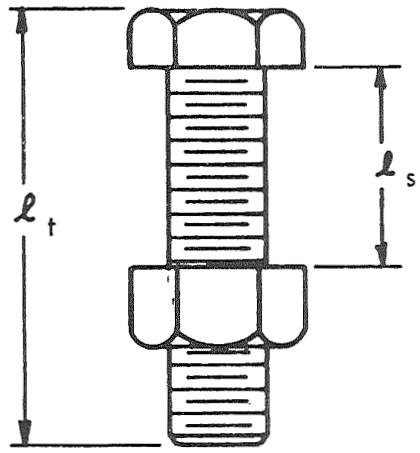

(1a)

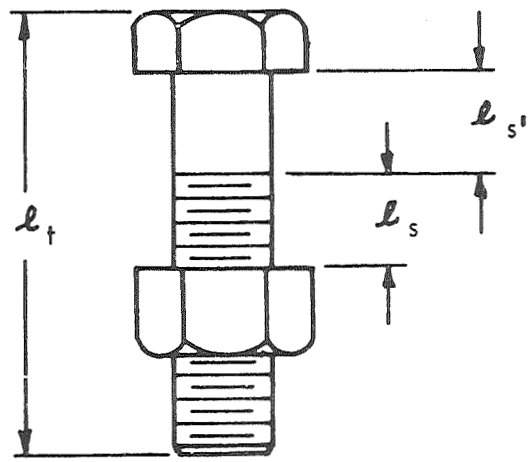

(1b)

Figure 4 - Bolt and Nut Diagrams Showing Relationships Between Total Length, ℓ_t, and Stressed Lengths, ℓ_s and $\ell_{s'}$, for Totally Threaded Bolts (1a) and Partially Threaded Bolts (1b).

At first, it might appear that a measurement of ΔF should be a convenient way of evaluating bolt loads, since the transit time does vary with load. The following discussion will show, however, that the accuracy of the method is quite limited. The round trip transit time in a 2 in. long bolt is approximately 20 μsec. Thus, ΔF_o is about 50 KHz. If the transit time is now changed from T_o to T_s by application of stress, the value of ΔF_s will change from 50 KHz by about 1 part in 10^2, or 500 Hz. However, the error associated with evaluating ΔF is also about 500 Hz. The accuracy can be improved somewhat by scanning across many nulls. If 10 nulls are scanned, the value of ΔF for the full scan would be 500 KHz, and the quantity $(\Delta F_o - \Delta F_s)$ would be about 5,000 Hz. For the 10 null scan, the error in evaluating the transit time, T_o, can probably be held to less than 1% but the error in evaluating $(T_o - T_s)$ still would exceed 10%. Thus, while ΔF measurements might help evaluate loads subsequent to the torquing operation, the accuracy will not be high and it will be necessary to keep precise records of the reference reading for each bolt. It will also be necessary either to make all measurements at the same temperature or to make adequate corrections for changes of temperature.

IV. FACTORS AFFECTING ACCURACY

The bolts which were examined during Phase I of this program are shown in Figures 5 and 6. Those shown in Figure 5 were supplied in limited numbers by the Marshall Space Flight Center and are further described in Table I. The bolts of Figure 6 were purchased locally in quantity for tests that required large numbers of specimens. Many of our preliminary tests were performed using the 3/4 in. aluminum bolt configuration shown in Figure 6 and designated MRI-1. Direct coupling of a transducer to the head of these bolts was made difficult by a small raised "bump" in the center. After removal of the bump with 400 grit paper, satisfactory echo patterns were achieved at a frequency of 10 MHz. Small commercial transducers were first coupled to the bolt head using silicone vacuum grease and a holding fixture as shown in Figure 7. Using this type of arrangement with the bolts loaded in a Skidmore-Wilhelm torque-tension tester, Δf-versus-load data were obtained similar to those shown in Figure 8.

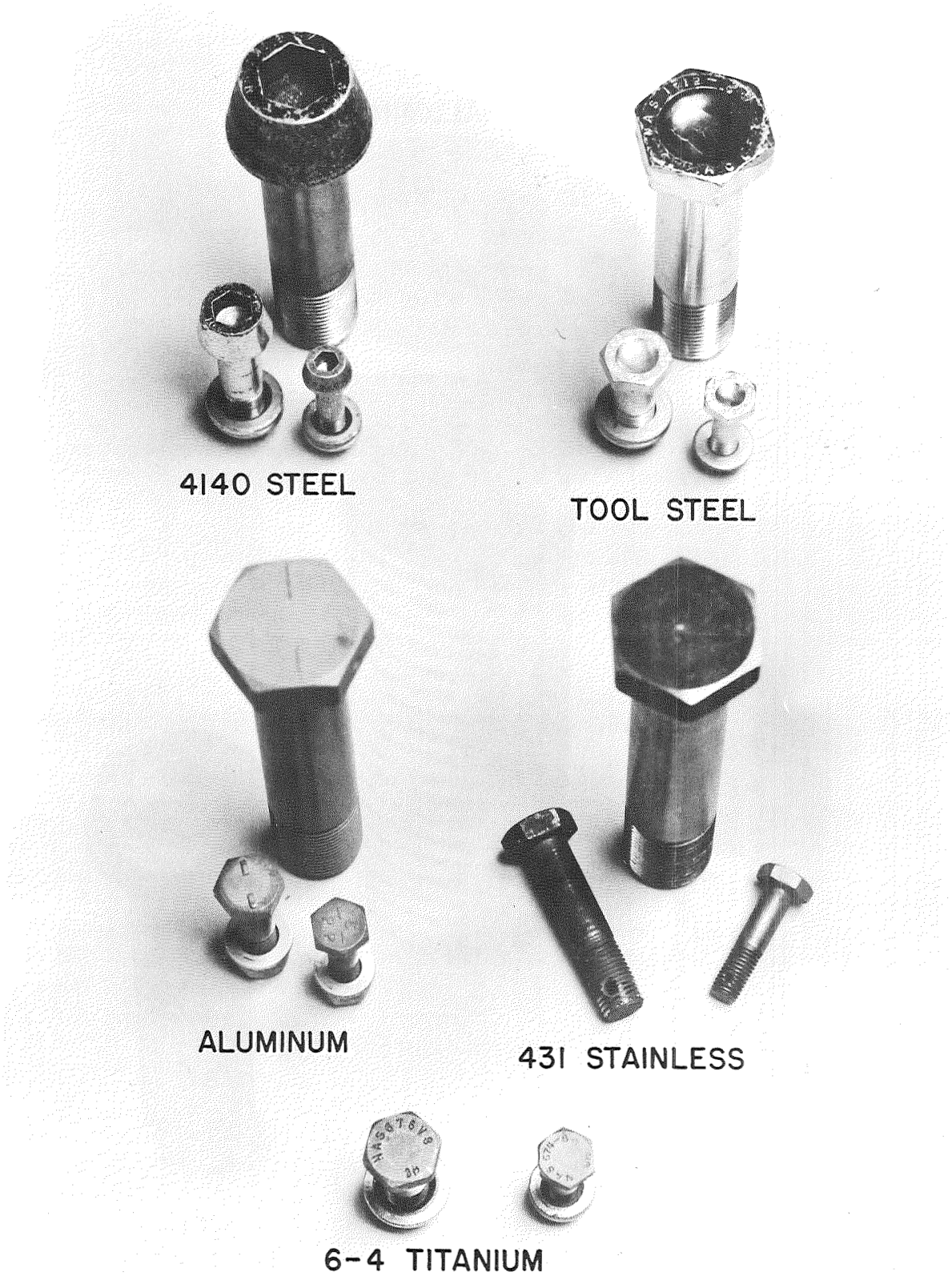

Figure 5 - NASA Supplied Bolts

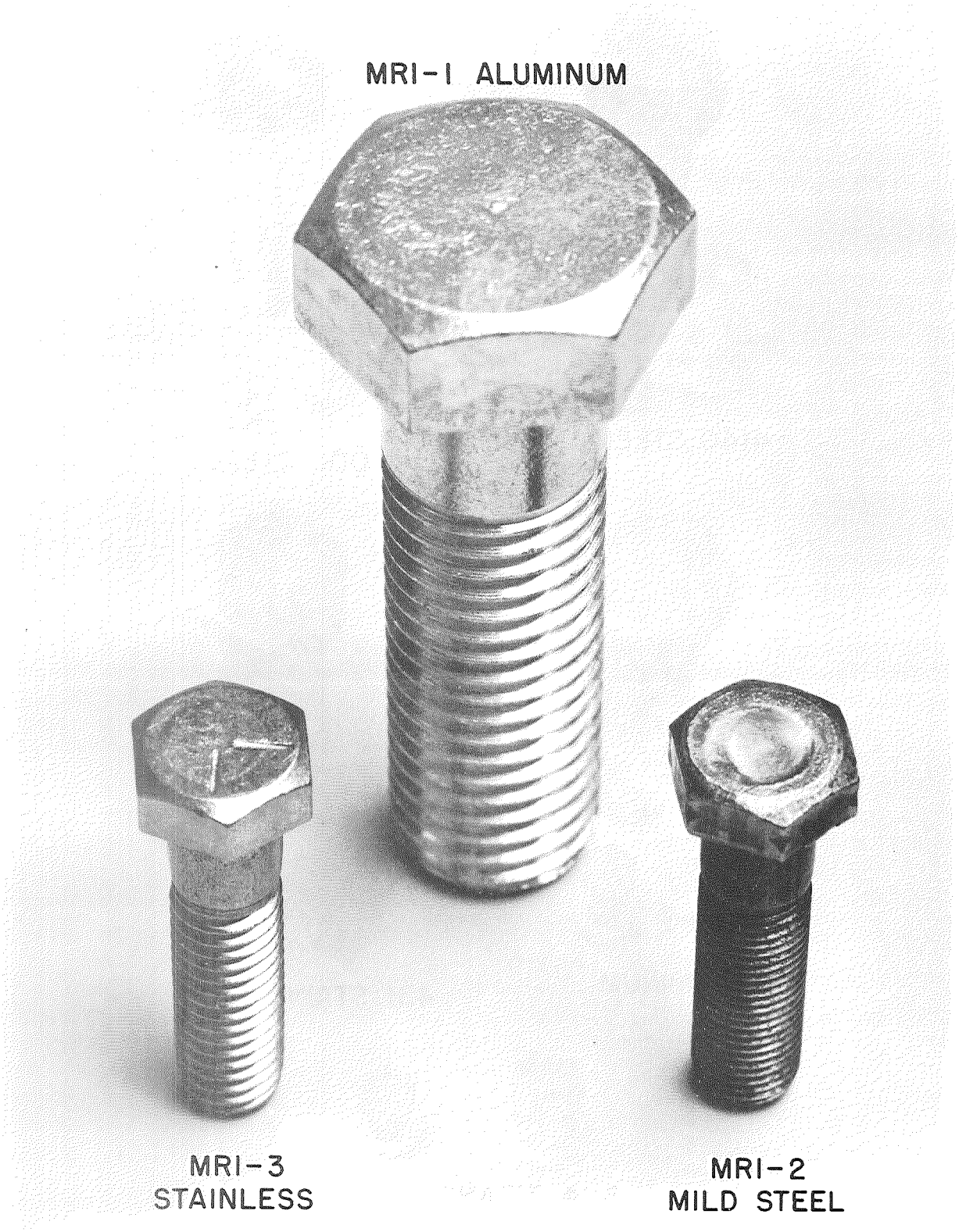

Figure 6 - Bolts Purchased Locally for Frequency Null Inspection

TABLE I

INFORMATION ON NASA BOLTS INVESTIGATED DURING PHASE I

Code Number	Size	Material	Ultimate Tensile Strength of Material	Configuration	Comments
NAS 676 V8	3/8 x 1.078	6-4 Titanium	~158,000 psi	Hex	
NAS 674 V8	1/4 x 0.925	6-4 Titanium	~158,000 psi	Hex	
AN 12DD-H35A	3/4 x 3.781	Aluminum	~ 60,000 psi	Hex	Drilled Head
AN 5DD-11A	5/16 x 1.219	Aluminum	~ 60,000 psi	Hex	
AN 4DD-10A	1/4 x 1.031	Aluminum	~ 60,000 psi	Hex	
AN 12C-36A	3/4 x 3.906	431 Stainless	~120,000 psi	Hex	
AN 6C-14	3/8 x 1.578	431 Stainless	~120,000 psi	Hex	Drilled Shank
AN 4C-10	1/4 x 1.032	431 Stainless	~ 120,000 psi	Hex	Drilled Shank
MS 20012-32	3/4 x 3.062	4140 Steel	~ 160,000 psi	Int. Wrench	
MS 20006-14	3/8 x 1.562	4140 Steel	~ 160,000 psi	Int. Wrench	
MS 20004-10	1/4 x 1.125	4140 Steel	~ 160,000 psi	Int. Wrench	
NAS 1312-29	3/4 x 2.853	Tool Steel	~ 160,000 psi	Hex	Spherically recessed heads
NAS 1306-12W	3/8 x 1.078	Tool Steel	~ 160,000 psi	Hex	
NAS 1304-8W	1/4 x 0.925	Tool Steel	~ 160,000 psi	Hex	
MRI-1	3/4 x 3.00	Aluminum		Hex	
MRI-2	3/8 x 1.75	Mild Steel		Hex	
MRI-3	3/8 x 1.75	Stainless		Hex	

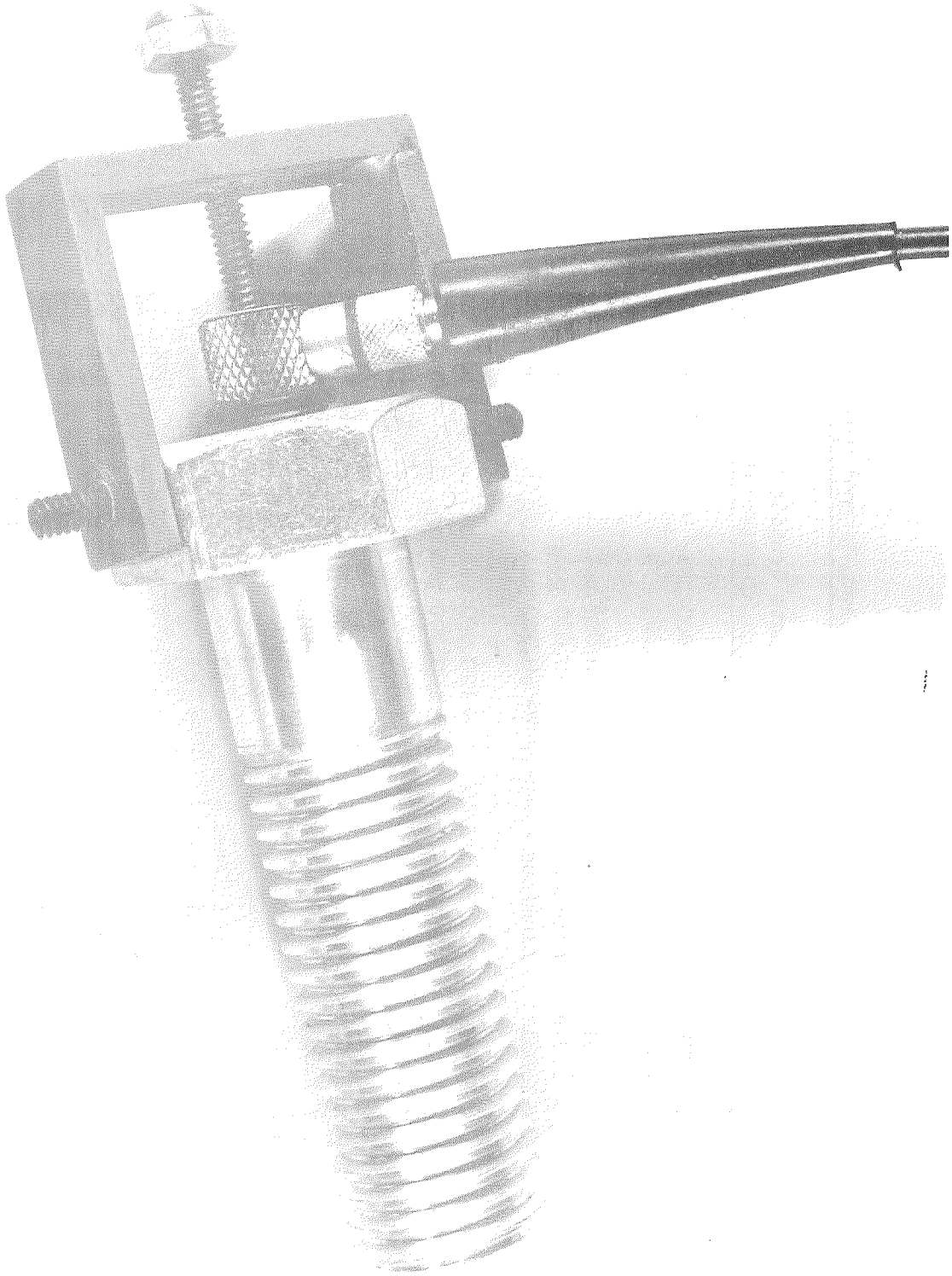

Figure 7 - MRI-1 Aluminum Bolt with Transducer Held in Place With Yoke Arrangement

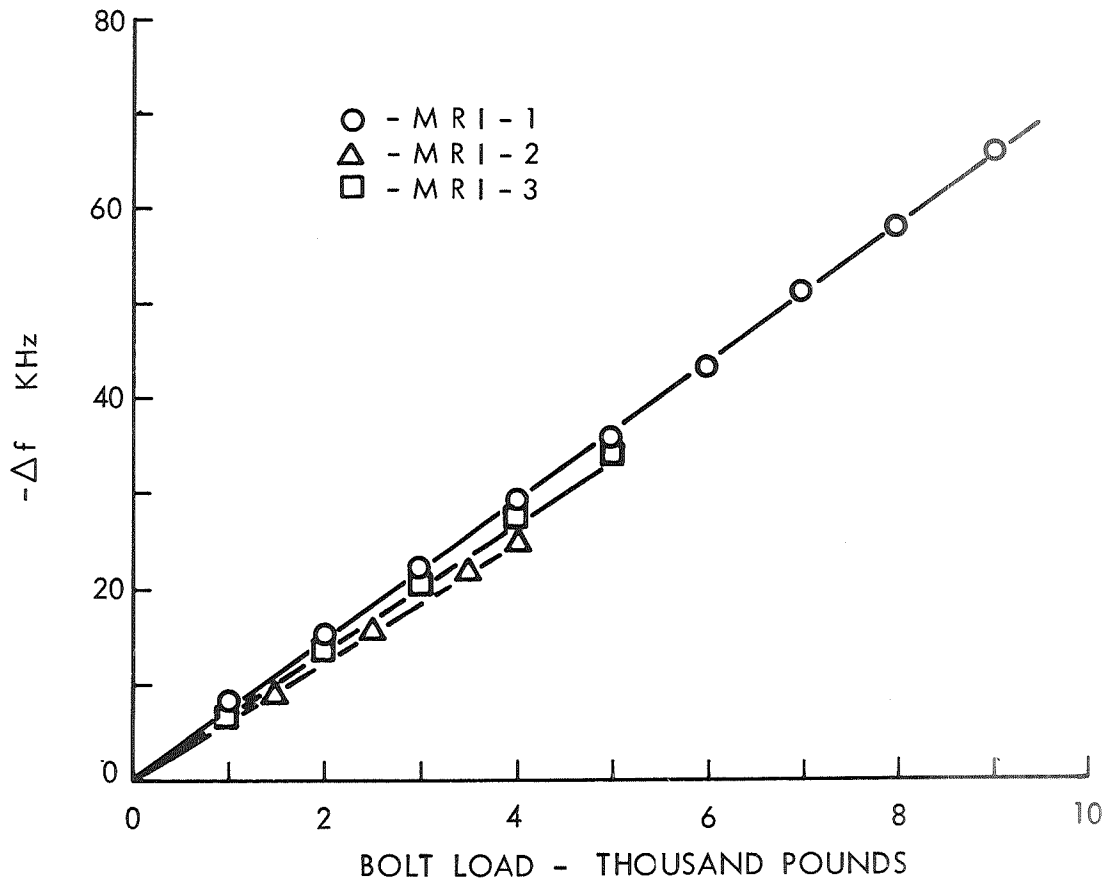

Figure 8 - Frequency Change Versus Bolt Load for Three MRI Bolts

The sign of Δf as indicated in Figure 8 is negative. Similar results were obtained for all of the bolts examined. Thus, as a bolt is loaded in tension the frequency of a given null decreases. This frequency decrease is in agreement with the increased length but, as mentioned previously, the sign of the velocity change is difficult to predict unless the so-called third-order elastic constants are known. This is not too important since we are not able to separate the effects of $\Delta \ell$ and Δv, but we have experimentally observed that the Δv effect is often larger than the $\Delta \ell$ effect and usually produces a decrease in f. Thus, the two effects are usually additive.

It can be noted from Figure 8 that for MRI-1 Δf is almost 70 KHz for a load of 9,000 lb., a reasonably typical load for this bolt. Since the null frequency at zero load and 9,000 lb. can each be reproduced to within 100 Hz, the reproducibility of Δf should be to within approximately 200 Hz, i.e., equivalent to an error of only about 0.3%. There are, of course, other factors which can increase this error but the measurement technique itself has high inherent accuracy. Some of the extraneous sources of error have been investigated and are discussed in the following sections.

A. Transducer Coupling

It is possible to couple ultrasonic waves from a transducer directly to an optically flat surface without any intermediate coupling agent. However, for the application at hand it is essential that some intermediate couplant be used. During this program numerous coupling methods were investigated including noncontact techniques with an intermediate water path, and contact techniques utilizing a wide variety of greases, oils, and water. The contact technique appears to be the most promising. Greatest reproducibility has been achieved using a silicone vacuum grease.

The grease couplant, of course, contributes to the round trip transit time of the ultrasonic signal. This contribution is small, generally much less than one period of the ultrasonic frequency, but it cannot be ignored in very precise measurements, especially if absolute values are of interest. Fortunately, such absolute measurements are not required in the frequency-null evaluation of load during assembly. As long as the thickness of the couplant doesn't vary during the bolt tightening process the bond contributes very little error to Δf readings. In fact, we have found that for a given bolt the transducer can be removed and replaced many times and the Δf versus load readings are reproducible to approximately $\pm$ 1%.

The effect of the couplant is much more troublesome when the ultrasonic load measurements are made subsequent to assembly. In this application we come closer to a need for absolute rather than relative measurements. Thus, the absolute frequency of a given null must change very little from one bond to another. This variation has been investigated and found to be about ± 3% on surfaces that are reasonably smooth and flat (about 60 μin. RMS or better). The reproducibility deteriorates with increasing surface roughness. Other factors, more important to the post-assembly load analysis problem, are discussed in Section VIII.

B. Bolt-End Geometry and Surface Condition

Optimum ultrasonic measurements are generally obtained on specimens with opposing surfaces flat and parallel. These ideal conditions cannot be expected in most bolts, so some indication of reproducibility is needed for non-ideal conditions. We have tried to obtain such data in a systematic investigation of both specially prepared and "as received" bolts. The results of this study indicate that non-parallelism of the bolt ends is less troublesome than we expected. Several aluminum bolts of MRI-1 configuration were prepared with the head and end surface out of parallel by various degrees. With non-parallelism ranging from 0 to 20 min., the Δf values for 10,000 lb. loads varied by only ± 1%. Some of these same bolts were then examined in the "as received" condition (except that the previously mentioned metal bump on the head was removed) and the data scatter was still less than ± 2%.

Statistical data were also obtained on some of the 3/8 in. mild-steel bolts (MRI-2) in the "as received" condition. Here the experiments were performed using a transducer-wrench tool in a way that simulated actual assembly procedures (see Section VI) and the scatter was ± 5%. The experiment was repeated on the same bolts after the ends were ground flat. The load values were then confined to a range of ± 2%. The grinding operation was performed by a hand-held technique, without any extreme care to insure parallelism. Based on the above results and subsequent examination of the bolts, it appears that accuracies are still satisfactory (± 5%) when the bolt surfaces are out of parallel by more than 1 degree.

Both of the bolt configurations mentioned above (MRI-1 and MRI-2) had simple hex heads that were reasonably flat. Many bolts have identification or alloy numbers stamped or embossed on the head. If such figures interfere with an intimate flat contact between the transducer and the bolt head, significant errors can be expected. The interfering characters must be avoided or removed if ultrasonic analysis is desired.

In the discussion on transducer coupling it was mentioned that a 60 μin. (RMS) surface finish gave satisfactory results. The coupling surface can probably be even rougher, approaching 100 μin. (RMS), but reproducibility will generally decrease with increasing roughness. The opposing surface, i.e., the threaded end of the bolt, can be somewhat rougher than the head. The threaded end only serves to reflect the ultrasonic waves back to the transducer and as such it only needs to be smooth enough to avoid excessive incoherent scattering. A finish of 200 μin. (RMS) or better is usually satisfactory.

C. Length

Expressions (1)-(3) clearly indicate that the slope of a Δf-versus-stress curve should depend on both the total length and the stressed length of a bolt. Experimental confirmation of this dependence was obtained through a series of experiments where the total length and the stressed length were varied. The results of one such experiment are shown in Figure 9. All of these data are from the same MRI-1 type bolt whose overall length was approximately 3 in. and whose stressed length was varied by changing the nut position along the threads. Between each set of data the stressed length was changed by approximately one revolution of the nut or 0.1 in. The load was applied hydraulically so that for a given nut position thread travel was eliminated during the loading cycle. It is quite clear that the slopes of the Δf-versus-load curves increase significantly as the stressed length is increased. Similarly, Figure 10 shows the effect of changes in total bolt length when the stressed length is held constant.

The above results emphasize that the stressed length and total length must both be known in order to determine the load or stress level represented by a given Δf value. However, the accuracy required in estimating these lengths is not great, so compensation should not be too difficult.

It should be recognized that some changes in the stressed length occurs during assembly. As the nut on a bolt is tightened by rotation, thread travel results in a reduction of the stressed length. Thus, the estimate of stressed length should be made for the desired state of stress. This can probably be done most easily by either direct calibration or from dimensional information about the parts to be fastened.

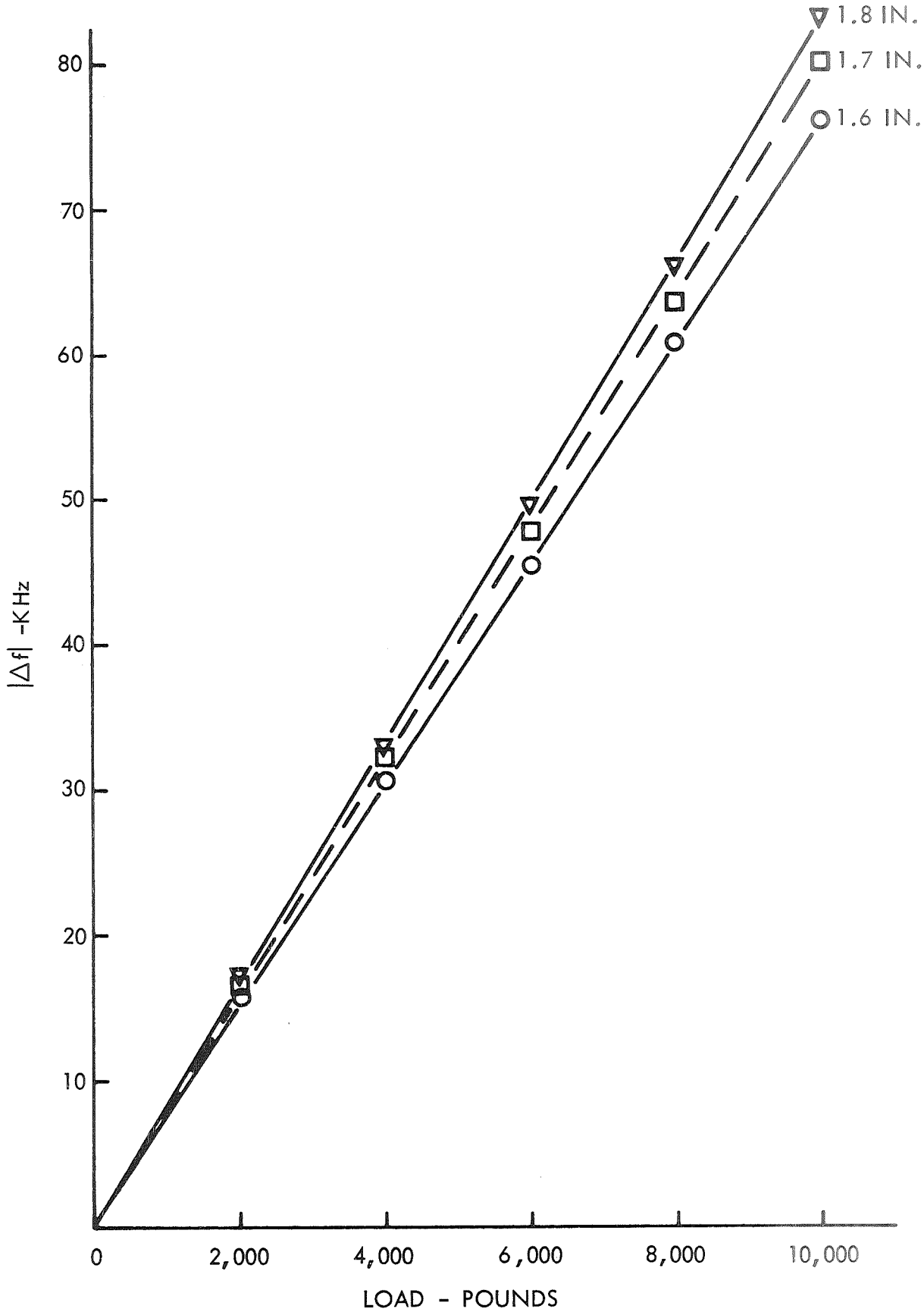

Figure 9 - Response Curves for an Aluminum Bolt With Indicated Stressed Length

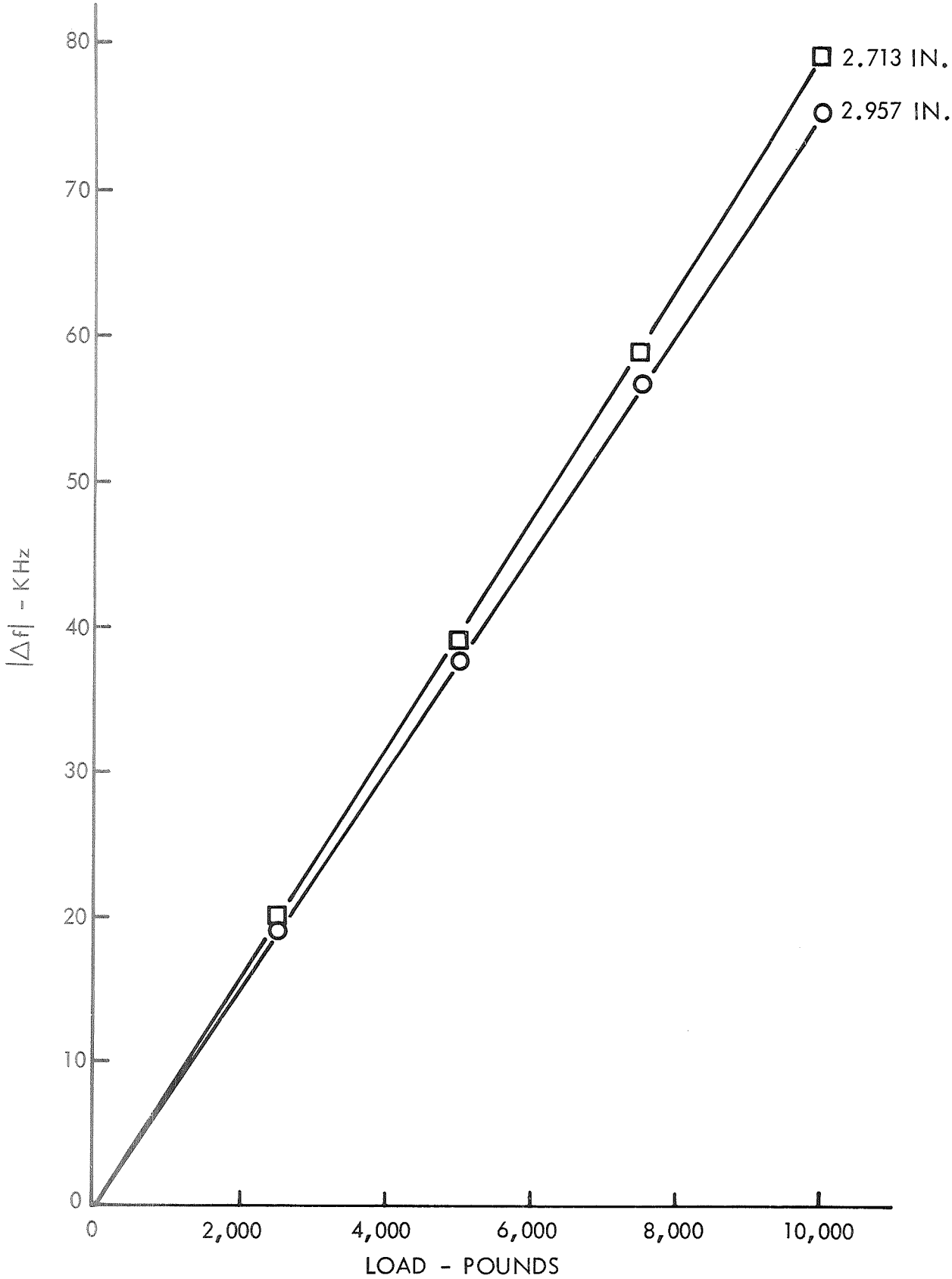

Figure 10 - Response Curves for Two Aluminum Bolts of the Same Stressed Length but With Different Real Length as Indicated

D. Temperature

Two different temperature effects were investigated as potential sources of error. The derivations of Appendix A clearly indicate that the frequency of a given null is dependent on any external variable which affects either the length of the bolt or the velocity of ultrasonic propagation. Temperature will affect both of these parameters. Figure 11 shows the effect of temperature on two of the bolts supplied by NASA. The frequency changes shown are due to temperature-induced changes in length and velocity. The slopes of the two curves are quite different, just as the Δf-versus-stress relationships are different for these same bolts. Over the temperature range represented in Figure 11 the change in frequency is by no means small when compared with the stress-induced effects. During the actual tightening of a bolt the expected temperature change will be quite small and can probably be neglected. To insure that this is the case, bolts should be at approximately the same temperature as the hardware in which they are utilized.

In contrast to the above, significant temperature changes are likely between assembly and post-assembly measurements. Thus, temperature corrections will definitely be required for any post-assembly load checks.

The second temperature effect investigated was the influence of temperature on the frequency-versus-load response. To examine this effect we studied an MRI-1 aluminum bolt at two temperatures which differed by almost 40°C. The results are shown in Figure 12. It is quite satisfying to see that the change in response over this relatively wide temperature range is quite small. In fact, the minor differences are probably due to a <u>change</u> in temperature that occurred <u>during</u> loading at the lower temperature. Thus, it appears that for assembly type measurements the temperature should present no serious difficulties so long as the temperature remains reasonably constant ($\Delta T \leq 1$°C) during the short period while the bolt is being tightened and the frequency null measurement is taken.

E. Plastic Yielding

For the data presented thus far, the bolt stresses did not exceed the yield strength. Thus, the unloading portion of a Δf-versus-load plot closely retraces the straight line load curve and returns to the initial condition. However, when the yield point is exceeded, the results are quite different, as illustrated in Figure 13. Plastic deformation causes the slope to increase rapidly (primarily due to the change in length) and prevents the unloading curve from retracing the loading curve. However, the entire unloading curve approximates a straight line with a slope almost equal to that of the elastic portion of the loading curve. The overall

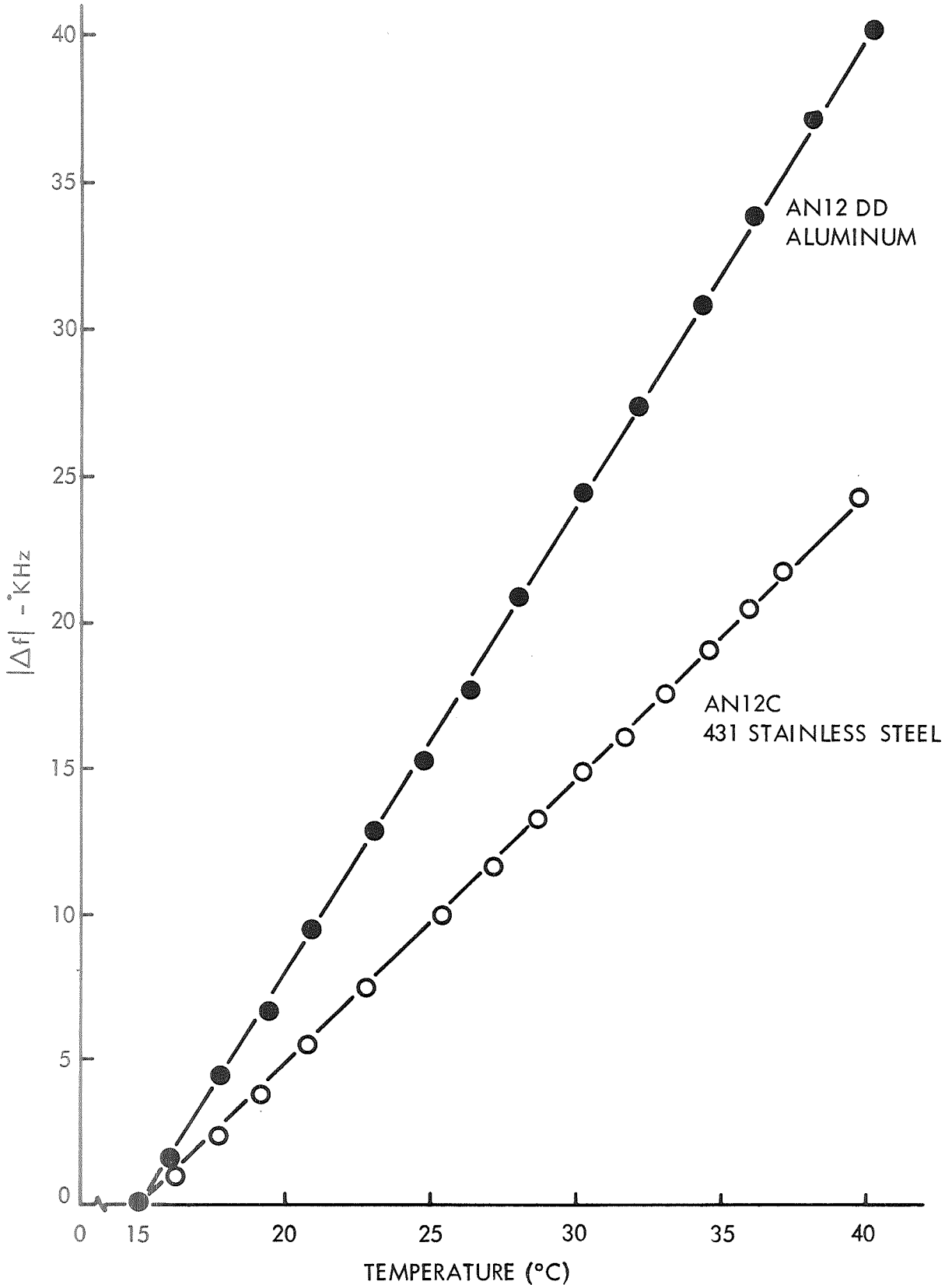

Figure 11 - Changes in Null Frequency Versus Temperature for Two NASA Supplied Bolts

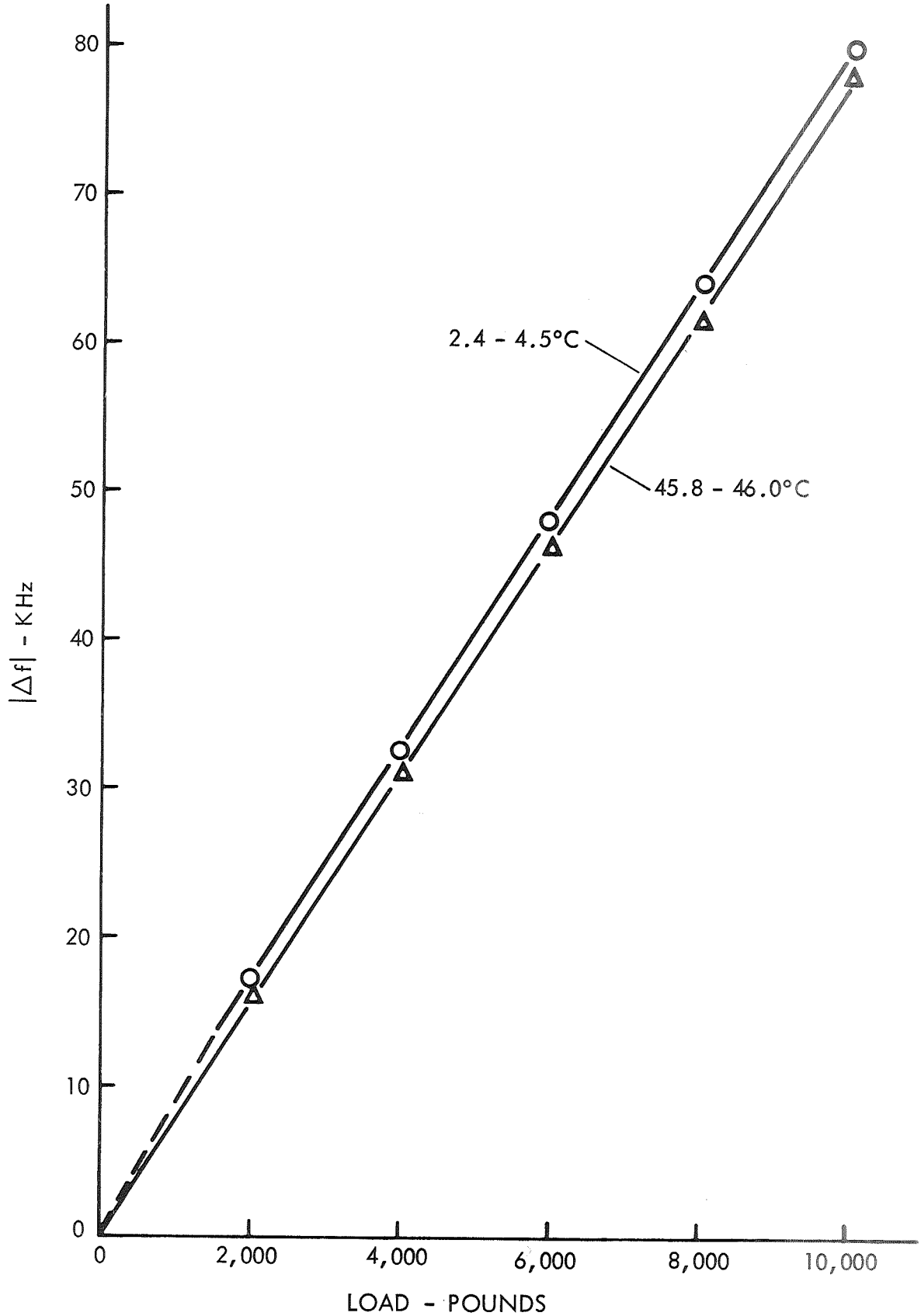

Figure 12 - Frequency Change Versus Load for an (MRI-1) Aluminum Bolt Held at the Indicated Temperatures During the Loading Operation

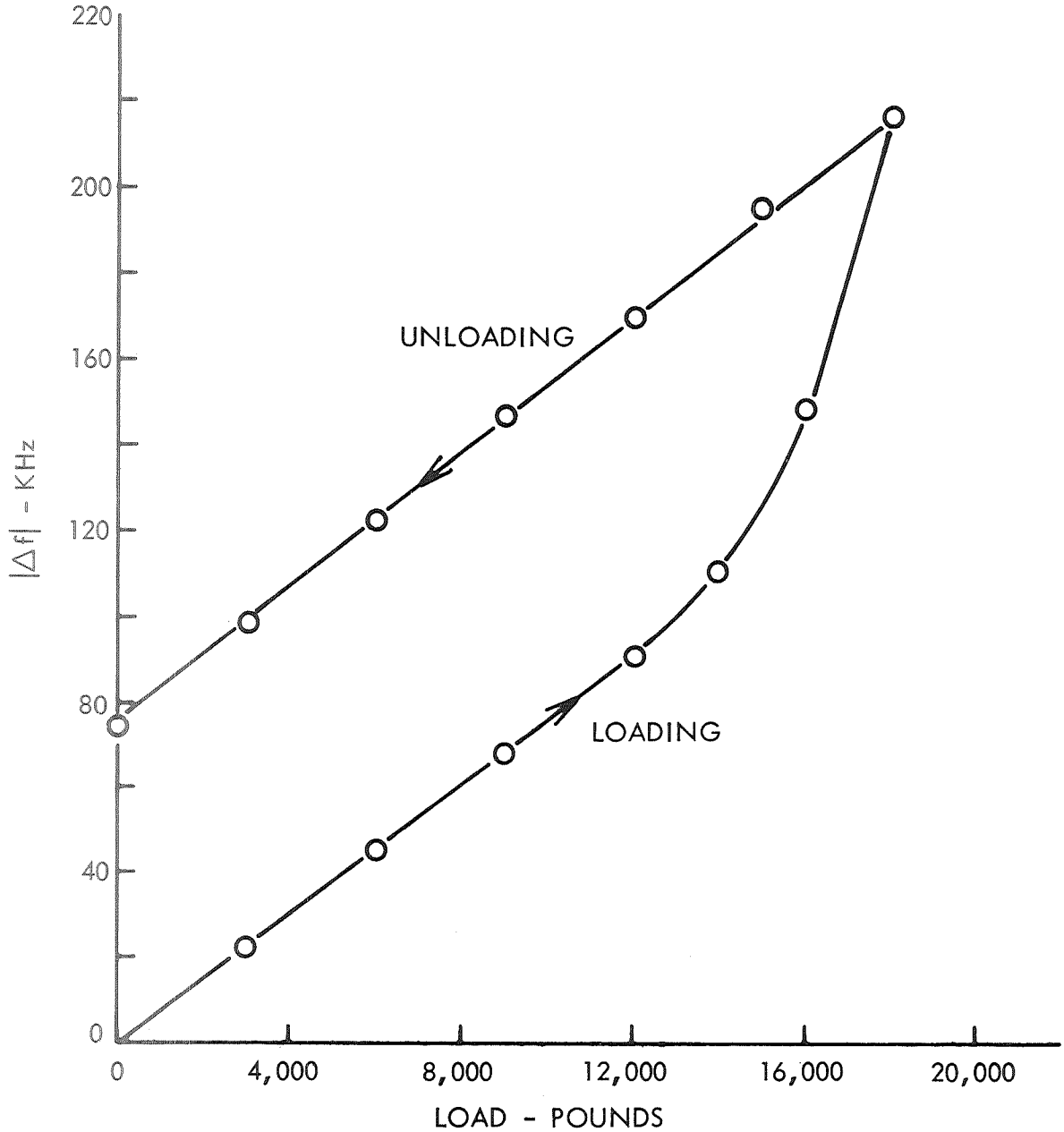

Figure 13 - Loading and Unloading Curves for an Aluminum Bolt Stressed Beyond the Yield Strength

response is very similar to that shown in an ordinary stress-strain curve where plastic deformation is present. Under these conditions, the frequency is multivalued in stress and ambiguity in stress analysis is therefore possible. However, it is also clear that the ultrasonic technique might be useful in detecting plastic deformation, a feature not easily detected with ordinary torque wrenches.

The effect of yielding was also investigated in an experiment in which three identical MRI-1 bolts were subjected to different loading conditions. The results are shown in Figure 14. All three bolts exhibited similar behavior in the elastic region but the extent of the region and the subsequent Δf response was clearly dependent on the loading condition. The bolts fractured at different tensile loads but they all fractured at approximately the same value of Δf, another feature which may be of value in the routine testing of bolts.

The above results indicate that plastic yielding shouldn't interfere with the anticipated use of the frequency-null technique in load analysis during assembly. In fact the technique should help in avoiding such yielding, which normally is undesirable. However, like temperature changes, excess stressing after assembly, during static firing for example, would change the pre-assembly reference length and make post-assembly analysis more difficult.

F. Shear Stresses

The effects of shear stresses on null-frequency measurements are also of interest and have received some attention. Some insight into this problem can be gained by re-examining Figure 14. Note that the Δf-versus-tensile-load response in the elastic region is very nearly the same for all three bolts even though two of them were loaded in torque tension. The torqued bolts were theoretically subjected to maximum shear stresses of approximately 18,000 psi at the upper end of the elastic region. The maximum shear stress level at this point is not too much less than the measured tensile stress.

Additional shear measurements were performed on bolts of both the MRI-1 and MRI-2 configuration. Frequency-null observations were made on the bolts while we attempted to apply pure shear stresses without any tensile load superimposed. In reality, some tensile stresses were probably present due to slight bending which was difficult to completely eliminate. The maximum shear stresses were of approximately the same magnitude as the tensile stresses which previously had produced Δf values of 30-70 KHz. Under nearly pure shear loading the observed Δf values were generally less than 0.7 KHz. Even this small effect was probably due to the slight bending

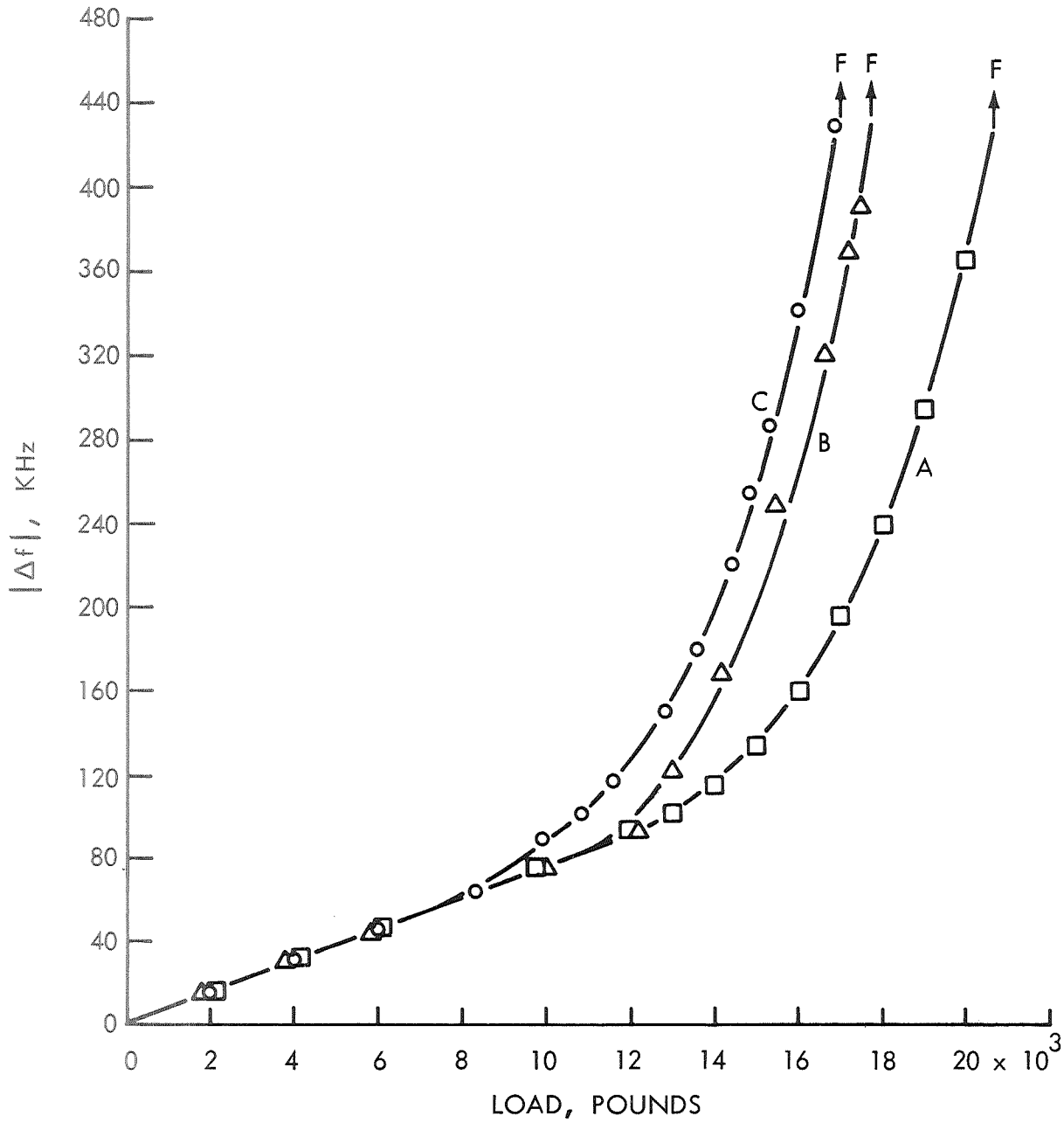

Figure 14 - Frequency Change Versus Load for Three Identical 3/4-In. Aluminum Bolts Loaded in (A) Pure Tension, (B) Torque-Tension with Threads Lubricated and (C) Torque-Tension Without Lubrication. Fracture, Symbol F.

mentioned earlier and discussed in more detail in the next section. Thus, it is our conclusion that pure shear produces an insignificantly small effect on the propagation properties of a longitudinal wave as used in our measurements.

G. Bending

Another source of error which was investigated is that of bolt bending during the tightening process as might occur in a variety of actual fastener applications. The condition was first simulated by placing steel shimstock under one edge of the bolt head during the loading process. The load was then applied hydraulically. The results of this test are shown in Figure 15. The straight-line response representative of nonbending conditions progressively degenerated as 10, 20 and 30 mil shimstock was placed under one edge of the bolt head. The results seemed to vary most widely under relatively light load conditions, and then to become somewhat more consistent at the higher loads. The test was not very quantitative but it emphasized the need for further study of the bending effect.

Further testing was accomplished by screwing a short segment of the threaded end of MRI-1 and MRI-2 type bolts into a rigid bar of steel. The bolt head was allowed to protrude from the bar surface by varying amounts. A transverse load was then applied to the head so that the bolt underwent bending in a cantilever mode. A transducer was coupled to the head and frequency-null observations were made during bending. Preliminary results indicated that Δf values of approximately 10 KHz could be created in either MRI-1 or MRI-2 bolts with bending moments of approximately 100 ft-lb. This was initially considered a rather alarming result because 10 KHz represents a very large error compared with the 30 to 70 KHz observed for ordinary tensile loads. Continued investigation revealed that Δf-versus-bending results were quite sensitive to the transducer position on the head of the bolt. We then discovered that the frequency of a given null would increase or decrease during bending depending on whether the transducer was displaced to one side or the other of the neutral fiber of the bending bolt. In addition, the magnitude of the Δf effect was observed to increase as the displacement from the neutral axis increased. With these results we were able to define the primary mechanism by which bending influenced frequency-null measurements. It is simply through the tensile and/or compressive stresses created by the bending. If a transducer is very carefully centered on the head of a bolt with an applied bending force, one-half of the ultrasonic beam travels in material under compression and one-half travels in material under tension. These stresses influence the incremental parts of the beam in exactly the same manner as an applied uniaxial stress. The overall result is that the ultrasonic wave front probably becomes non-planar, or its orientation at least changes with propagation; thus the wave

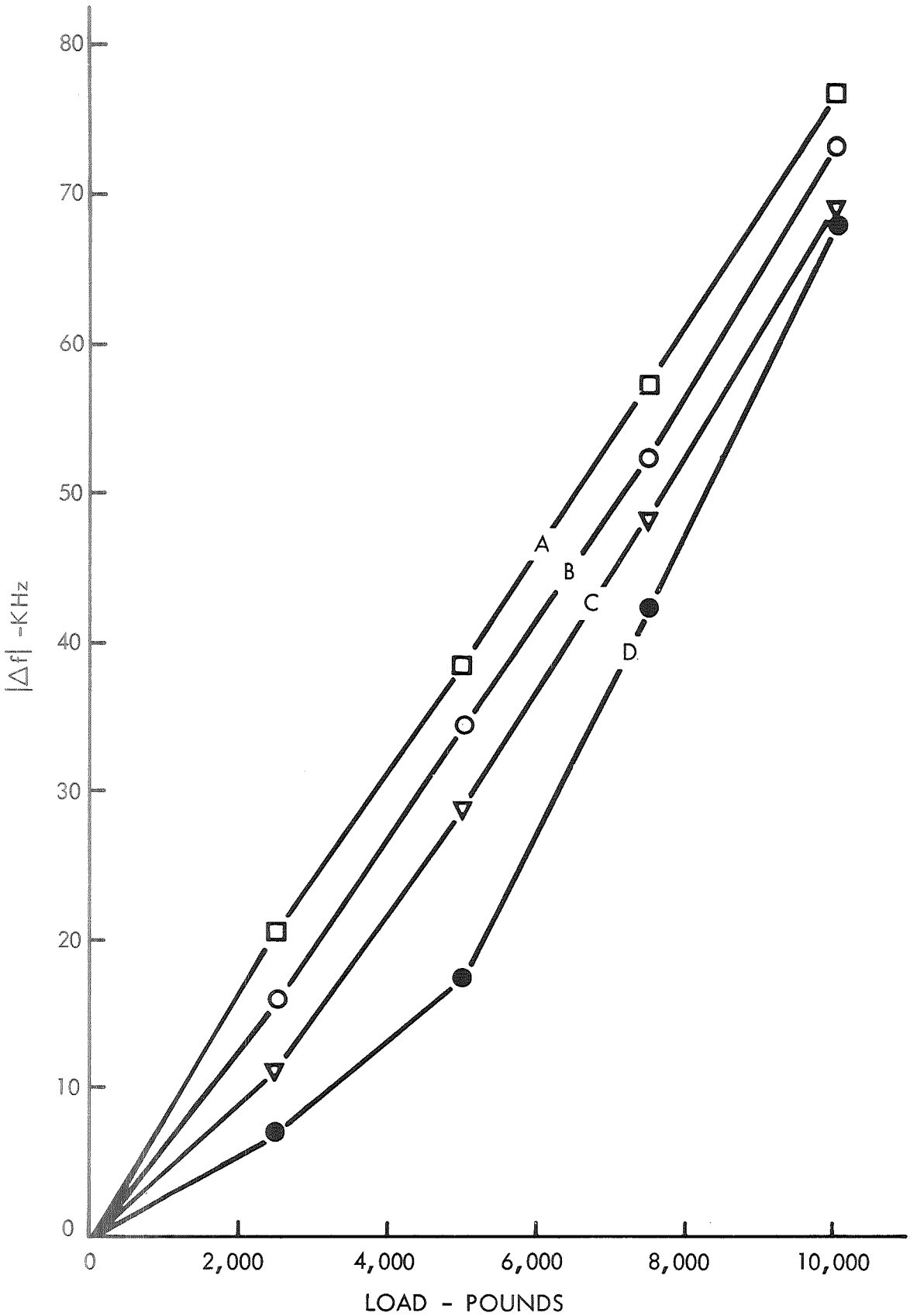

Figure 15 - Frequency-Versus-Load Curves for an Aluminum Bolt With (A) 0 Mils, (B) 10 Mils, (C) 20 Mils, and (D) 30 Mils of Steel Shimstock Under One Side of the Bolt Head to Induce Bending During the Loading Operation

front of a returning echo is not completely parallel to the transducer surface. The electrical signal created by such a wave will be phase shifted from the condition represented by no bending. The magnitude of the phase shift increases from the no-bend condition as the beam is displaced further from the neutral axis.

With the above mechanism active it is clear that frequency-null measurements may exhibit considerable scatter if bending is present. The errors due to bending can be minimized by centering the transducer on the neutral axis and, with care the total scatter in a series of tests can be held to a few percent. Nevertheless, bending does present one of the largest sources of data scatter. The reason for this becomes quite clear by observing that the maximum fiber stress, in bolts subjected to a bending moment of 125 ft-lb, may exceed the recommended tensile stress. The stresses due to bending are, of course, superimposed upon any tensile stresses due to bolt tightening and the resultant stresses are very inhomogeneous. Although frequency-null measurements may exhibit data scatter related to the inhomogeneous stresses, it must be recognized that these frequency variations are indicative of true stress variations. If these variations could be monitored by some yet to be developed multiple transducer technique, it might be possible to ultimately evaluate bending effects also.

V. NASA SUPPLIED BOLTS (Phase I)

Of the NASA supplied bolts, shown in Figure 5, the head configurations varied considerably. Because of embossed identification characters and complex heads, one bolt of each type (except those made of 4140 steel) was first prepared by machining the head and threaded ends flat and parallel. For bolts which contained drill holes in either the head or shank, sufficient material was removed to eliminate the hole. The 4140 steel bolts were not prepared in this manner because of the internal wrench head; however, the bottom of the wrench hole was flattened with an end mill. These rather idealized conditions were created in order to evaluate the Δf-versus-load characteristics of each bolt without undue influence from extraneous geometrical factors.

The Δf-load characteristics of the four 3/4 in. bolts are shown in Figure 16. Although the data presented in Figure 16 have not been normalized to a constant value of ℓ_s/ℓ_t , such a correction would not effect a major change in any of the four response curves. Aluminum is obviously the most sensitive material with the three steels all exhibiting significantly smaller slopes.

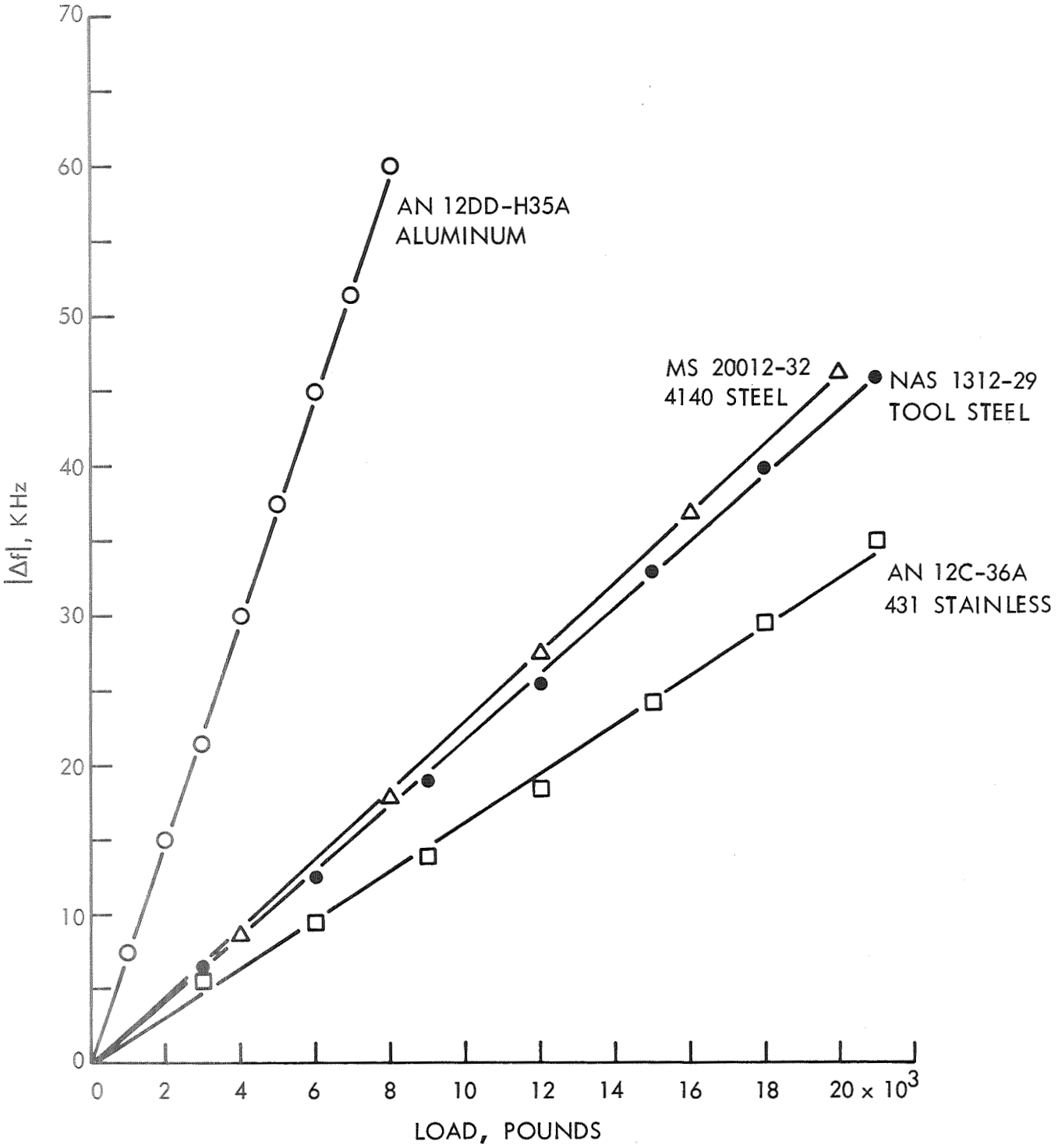

Figure 16 - Frequency Change Versus Load for Four NASA Supplied Bolts. All are 3/4-in. bolts with head and threaded ends machined flat and approximately parallel.

The response curves for three of the smaller bolts are plotted in Figure 17. Even in these smaller bolts reasonably satisfactory results were obtained by simply using silicone vacuum grease to couple the housed transducer to the bolt head. Using this technique we were able to examine all of the NASA supplied bolts (after end machining) except MS 20004-10, the 1/4 in. bolt with an internal wrenching head. After testing different size bolts of each alloy, the load data were converted to stresses and the curves of Figures 18 and 19 were obtained. For each of five alloys, Δf is plotted against several calculated stress levels to which each bolt was tested. Theoretically, all of the data points should fall on a straight line passing through the origin. However, some deviation from this ideal can be traced to the fact that all stress calculations were based on the diameter of the bolt shank and no consideration was given to the two stress areas discussed earlier in this report. Under these conditions the results are rather impressive. It is desirable to achieve good agreement of Δf-versus-stress for different bolts of a given alloy because this will facilitate the extrapolation of a single calibration test to bolts of widely varying sizes. A more detailed study of this problem is included in Section VII.

VI. PROTOTYPE INSTRUMENTATION

During Phase II of this program, prototype instrumentation was assembled and checked out. This equipment, to be delivered to the Marshall Space Flight Center for further testing and evaluation, includes an electronics console, cables, transducers, and a few hardware items which facilitate testing bolts with a variety of head configurations. We believe that this equipment is the best solution to the bolt load analysis problem within the available time and funds of the project. Much of the electronic package was assembled from commercially available components. Certain modifications and additions, which would facilitate operation, are discussed later in this Section.

Figure 20 is a photograph of the prototype equipment being used to set bolt pre-loads. A block diagram of the prototype is shown in Figure 21. In this equipment, the 1,000 Hz calibration signal from the oscilloscope is used to trigger the gated amplifier and to control the pulse repetition rate. The signal generator provides a variable frequency CW signal to the inputs of the gated amplifier, the frequency counter, and the phase detector. The rf pulse output from the gated amplifier drives the transducer. The resultant signals from the pulse-echo train pass through the phase detector module, which in turn provides two separate signals to the double channel oscilloscope. Channel B of the scope displays the unrectified rf pulse-echo train and Channel A displays the same pulse-echo train after phase detection.

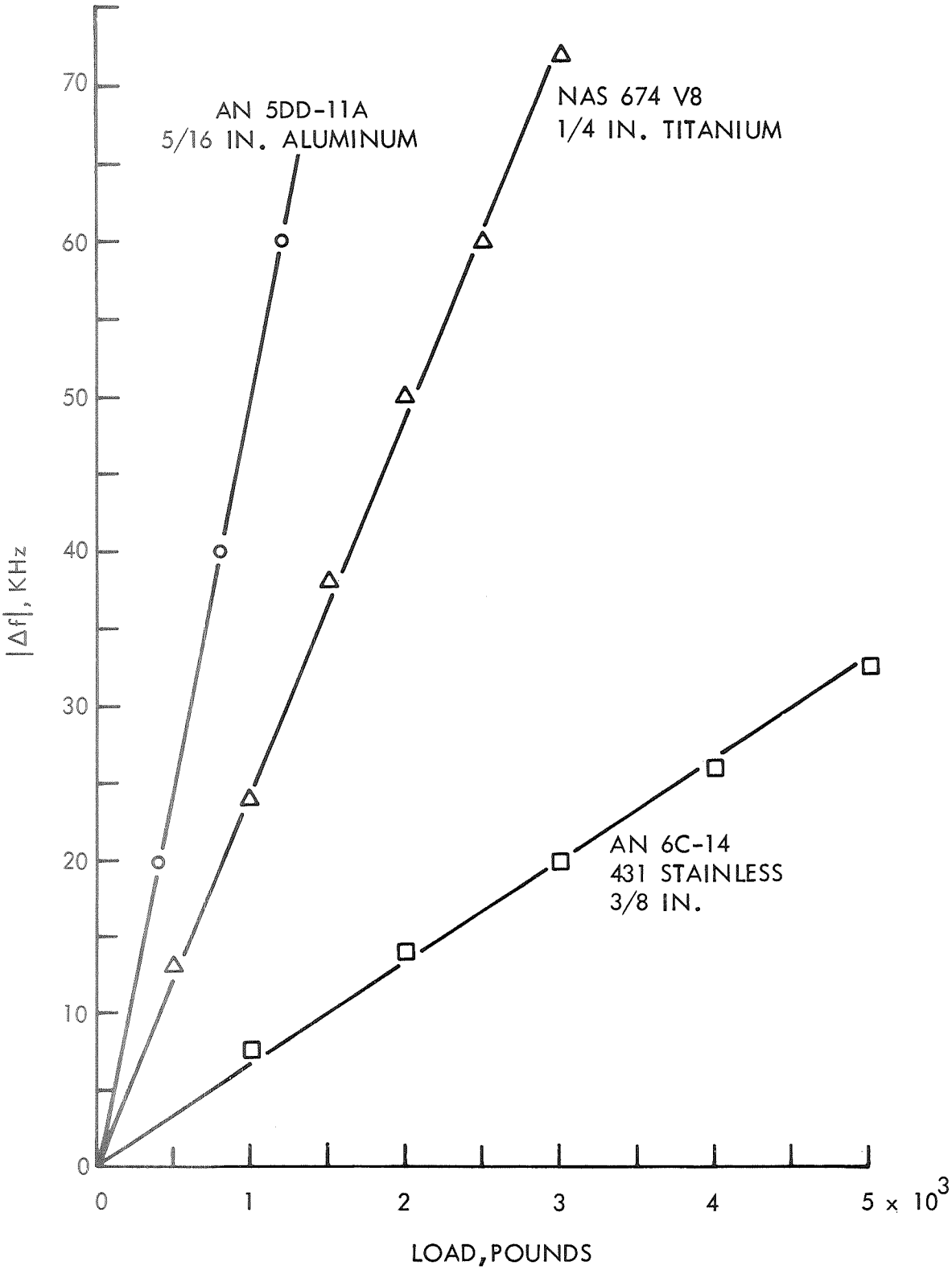

Figure 17 - Frequency Change Versus Load for Several Different Bolt Sizes and Alloys. Head and threaded end were machined flat and parallel on all bolts.

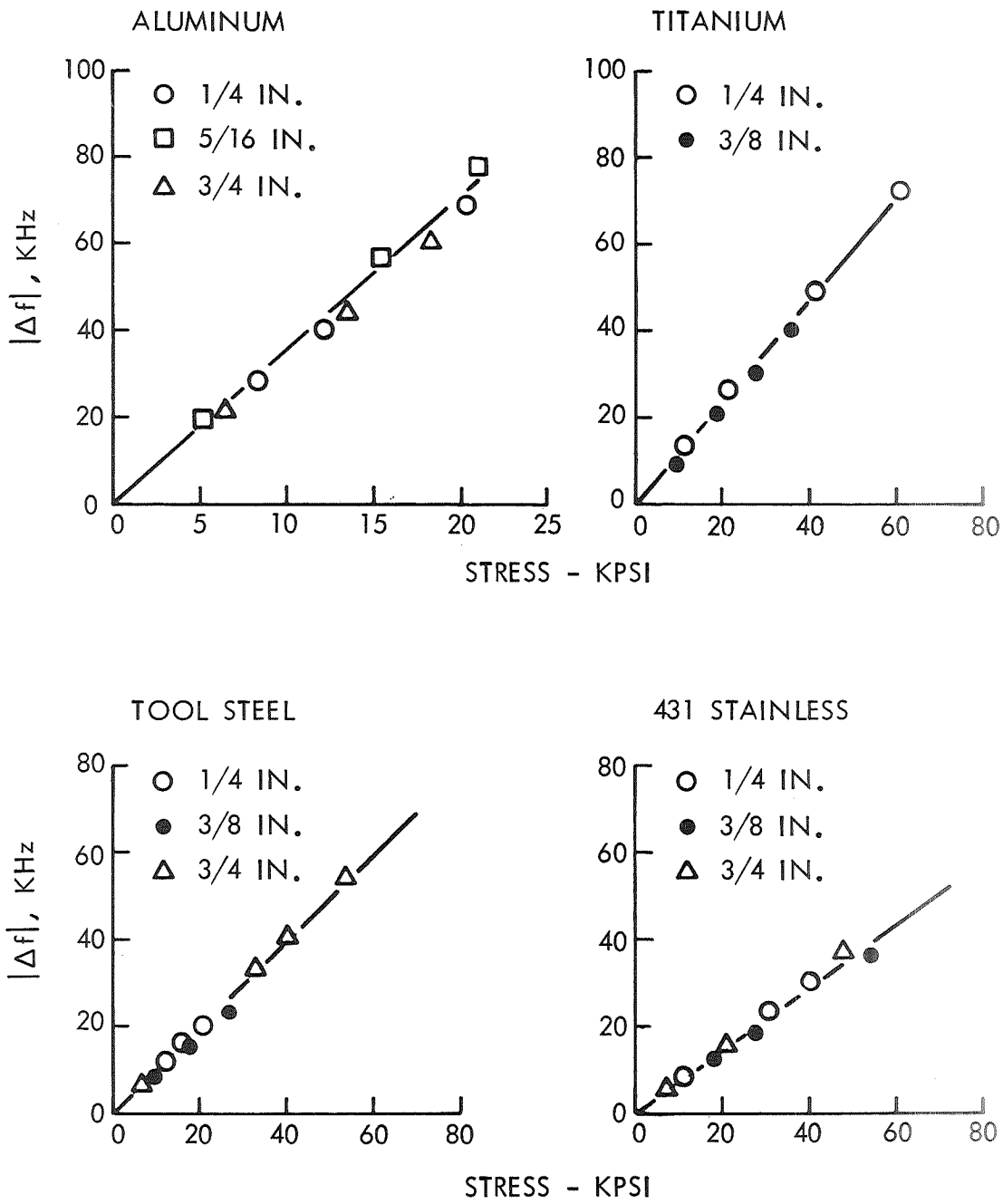

Figure 18 - Normalized Frequency Change Versus Stress for NASA Supplied Bolts. Head and threaded ends were machined flat and parallel.

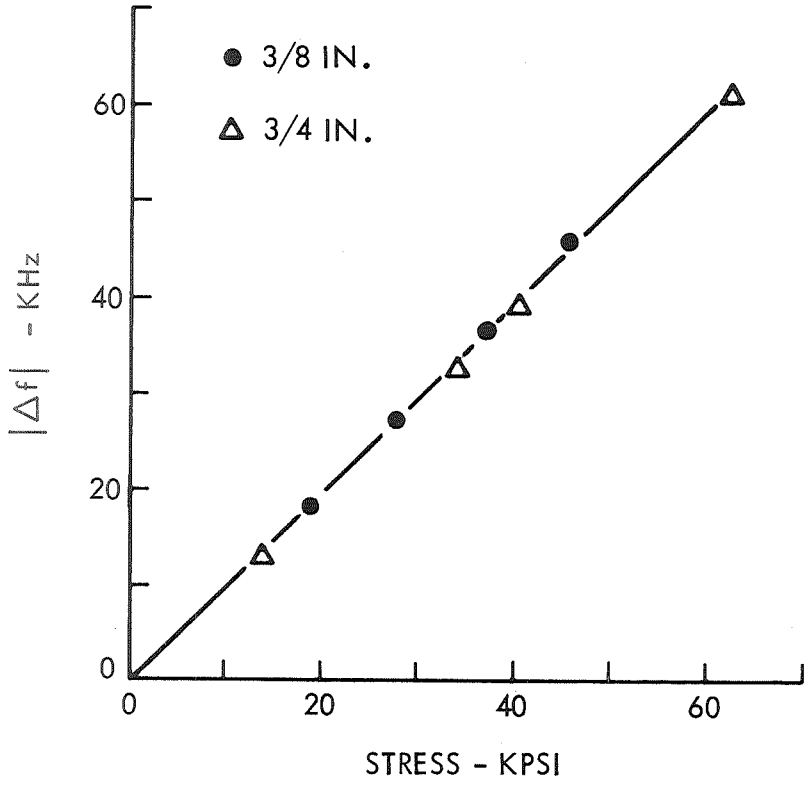

Figure 19 - Frequency Change Versus Stress for 3/8-In. and 3/4-In. Bolts of 4140 Steel.

Figure 20 - Photograph of Prototype Instrumentation Being Used to Set Bolt Preloads on a Vacuum System.

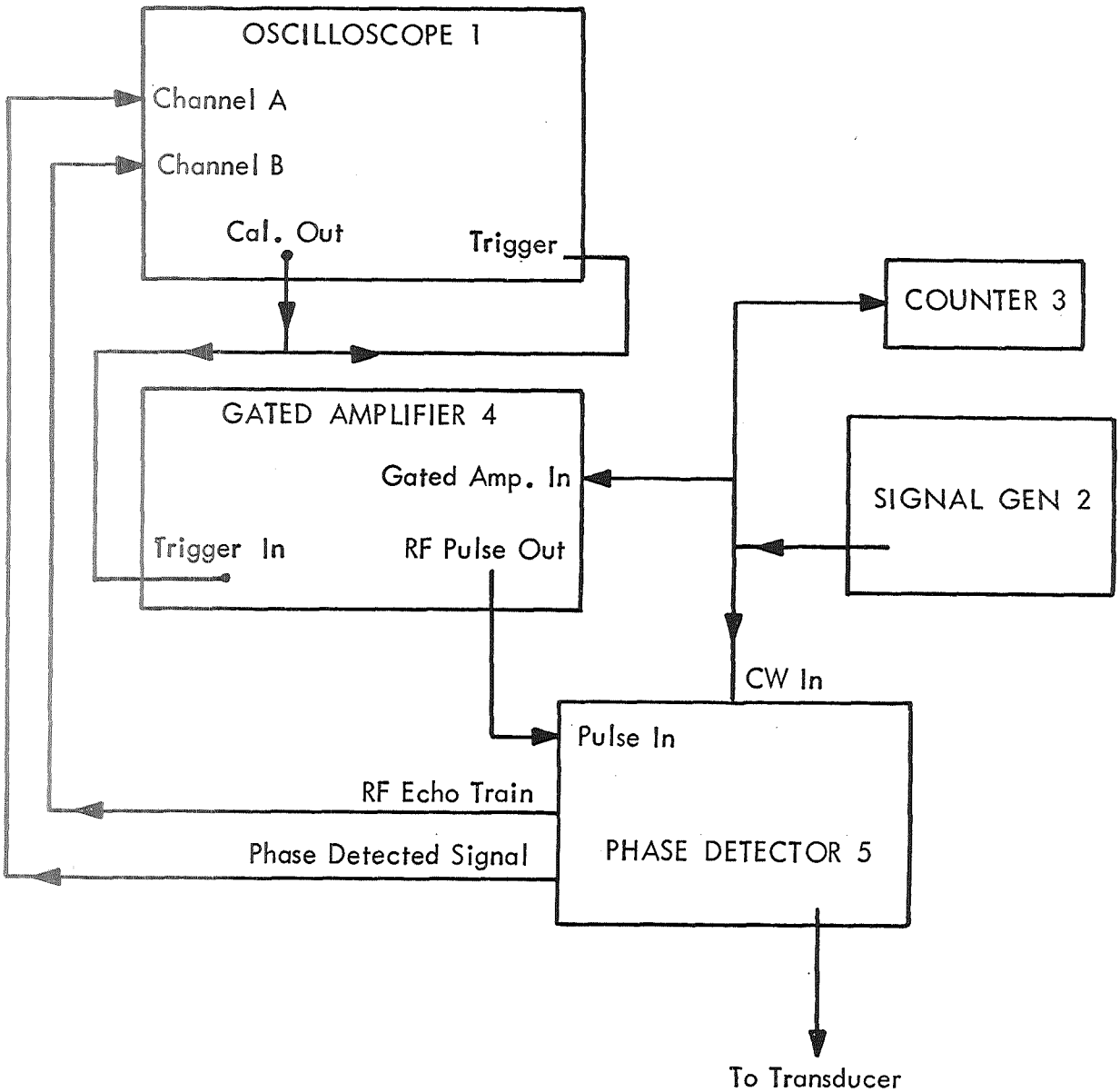

Components are Identified as Follows;

1. Tektronix Oscilloscope Model 561B
2. Krohn-Hite Oscillator Model 4200R
3. Eldorado Frequency Counter Model 325A (Modified)
4. Arenberg Ultrasonics Lab Model PG650C Mod. IIJb
5. MRI Made Phase Detector

Figure 21 - Block Diagram of Prototype Fastener Load Analyzer

A more detailed description of the prototype equipment and the procedure of operation are included in the Technical Manual. However, a brief outline of the operating procedure is included here for the sake of completeness. After the equipment is warmed up, a suitable transducer is applied to a bolt head and the pulse-echo train is observed on Channel B of the scope. Two oscillograms from different bolts are shown in Figure 22 with Channel B displayed as the lower trace in each case. The first echo is identified and the sweep and horizontal position controls are adjusted until the first echo is near mid-screen. The frequency is then adjusted until the phase detected signal corresponding to the first echo is either a positive or negative peak and the position controls are once again adjusted until these peaks are exactly at mid-screen (or any other convenient graticule line). Figure 23 includes several oscillograms which show the phase detector output indicating different phase angles between the CW reference signal and the first echo signal. In reality, the phase detector signal can be set to any convenient condition for reference purposes but we suggest the null condition corresponding to $\varphi = 90$ degrees (Figure 23b). (Note that the $\varphi = 90$ degrees null condition is usually distinguishable from the $\varphi = 270$ degrees null (Figure 23d) by the slope of the trace crossing the graticule line.) Figure 24 shows another series of oscillograms from a stainless steel bolt.

After a reference phase condition is set by manual adjustment of the signal generator, the frequency, f_o , is noted by reading the digital counter. Then, by using prior calibration data the operator determines the frequency change, Δf , corresponding to the desired load condition. The value of Δf is subtracted from f_o and the signal generator is reset until the counter reads the frequency $f' = f_o - \Delta f$. This adjustment of the frequency, of course, destroys the reference phase condition, which must be reestablished by loading the bolt. Thus, during the tightening operation the operator simply observes the Channel A scope presentation until the reference phase condition is reestablished.

Some care must be exercised when using the above procedure in examining long bolts. In Section III it was mentioned that if the frequency is changed by ΔF the interferometer goes from the nth null condition to the $(n \pm 1)$ null condition. Since $\Delta F = 1/T$, where T is the round trip transit time, we find that for fairly long bolts ΔF may be smaller than the desired Δf . Thus, when the operator adjusts the frequency from f_o to f' the phase angle, φ , may change considerably more than 360 degrees. If this happens the operator must observe exactly how many times, N , the reference phase condition occurs during the frequency adjustment. Then, as the bolt is tightened the system is returned to the reference phase condition by counting through N nulls. This procedure is analagous to that of counting fringes in an optical interferometer. For a bolt 6 in. long a typical value of ΔF might be 20 KHz. For high strength steel, such as A286, the value of Δf could exceed 150 KHz. Thus, N would be at least 7.

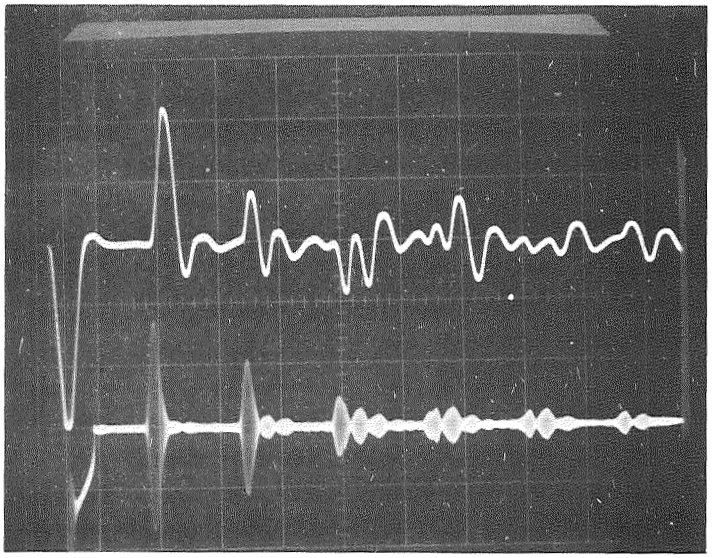

(a)

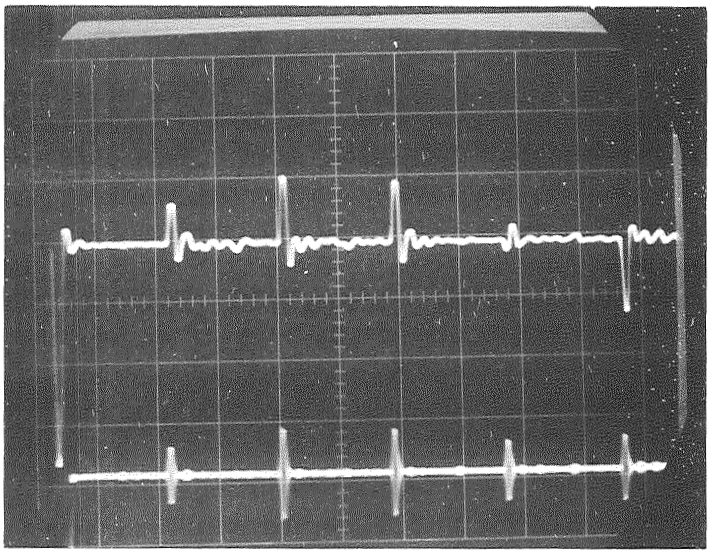

(b)

Figure 22 - Oscillograms Showing Scope Presentation From (a) a 3/4-In. 431 Stainless Steel Bolt (AN 12C-36A) and (b) a 5/16-In. Aluminum Bolt (AN5 DD-11A). The bottom trace in each oscillogram is the unrectified pulse-echo pattern. The top trace is the output from phase detector.

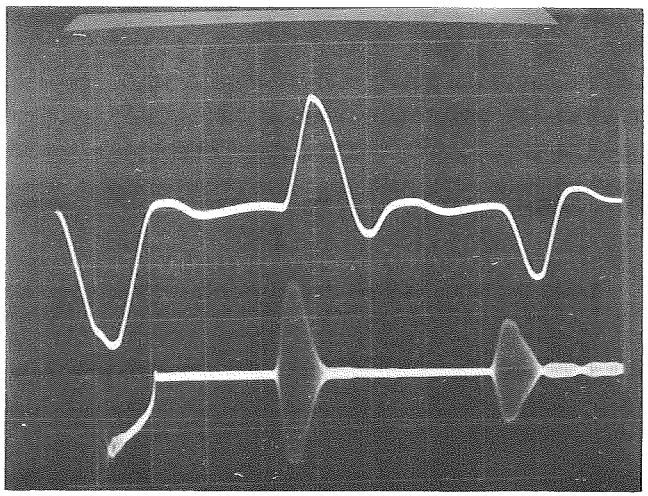

(a)

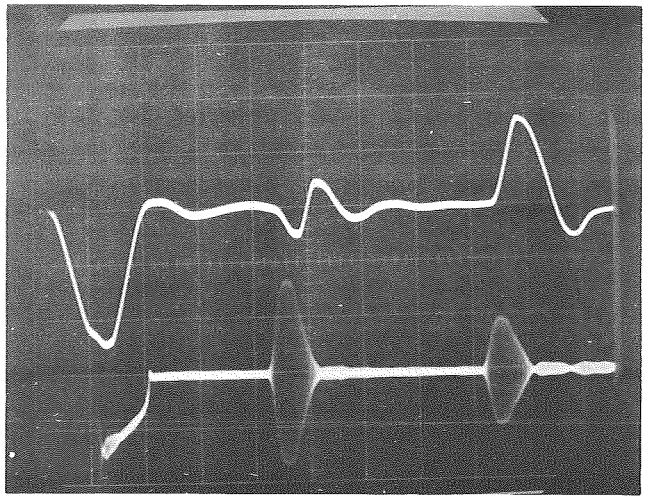

(b)

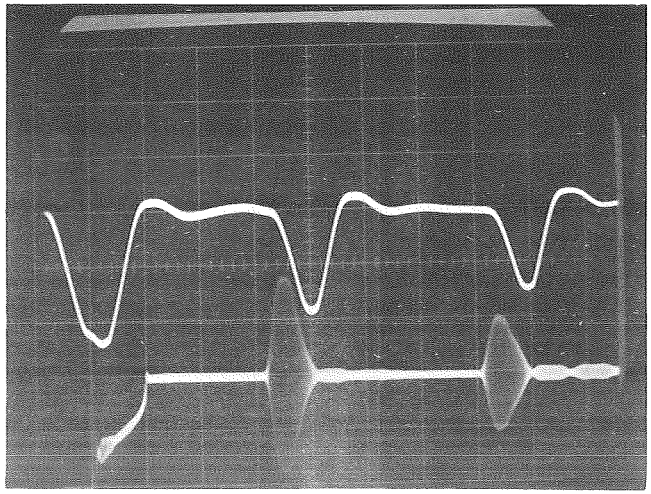

(c)

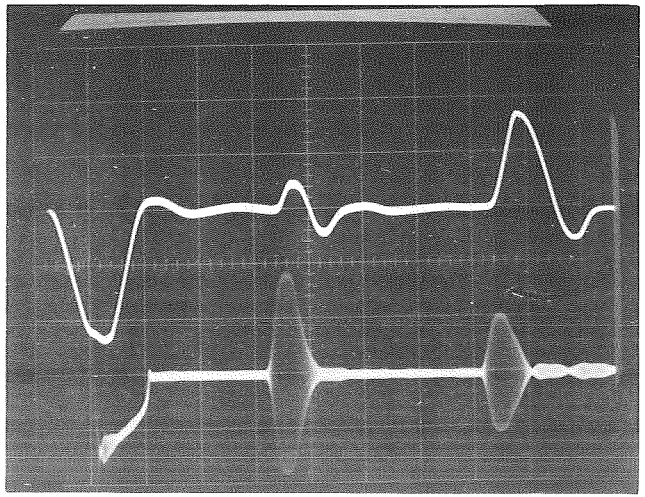

(d)

Figure 23 - Oscillograms From a 5/16-In. Aluminum Bolt (AN5 DD-11A) With the Phase Detected Signal (Top Trace) of the First Echo Centered in the Horizontal Direction. The frequency was adjusted to produce varying phase angles between the first echo and the CW reference signal. The approximate phase angles are (a) 0 degree, (b) 90 degrees, (c) 180 degrees, and (d) 270 degrees.

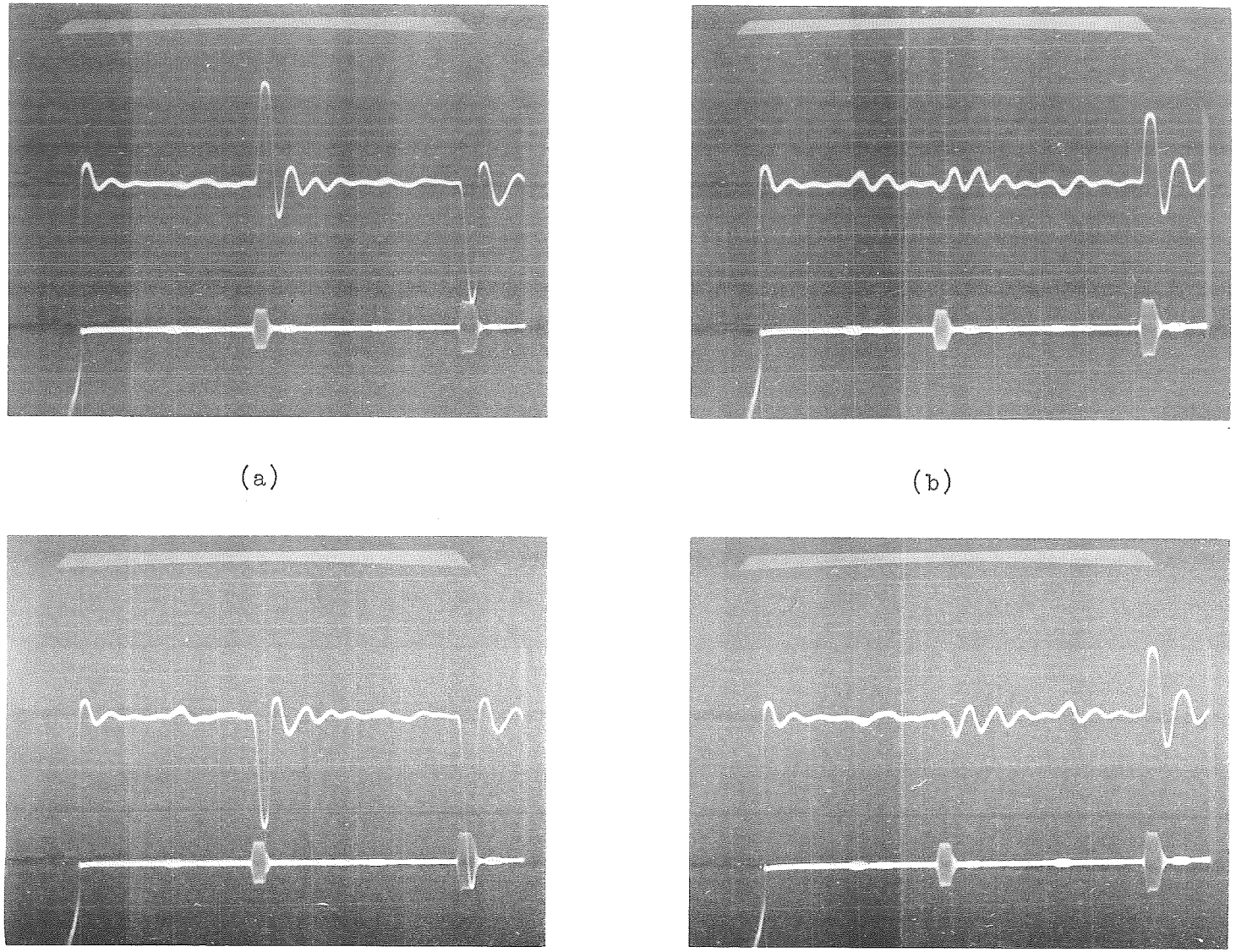

Figure 24 - Oscillograms From a 3/4-In. Stainless Steel Bolt (AN 12C-36A) With the Phase Detected Signal (Top Trace) of the First Echo Centered in the Horizontal Direction. The frequency was adjusted to give varying phase angles between the first echo and the CW reference signal. The approximate phase angles are (a) 0 degree, (b) 90 degrees, (c) 180 degrees, and (d) 270 degrees.

We have found that the above effect causes little difficulty, especially when numerous bolts of a particular description are being used. The value of N is easily established during evaluation of the first bolt. This same value is applicable to all similar bolts used in the same application.

There are several additions or modifications which could be made to facilitate operation of the prototype equipment. For example, a gating circuit and signal level monitor could be included to automatically maintain a given null condition during the preloading operation. With this type of system the operator could simply set the reference null condition and note the frequency, f_o. Then as the bolt preload is applied the signal level monitor would maintain the null condition by providing an error signal to a servo-controlled oscillator. The latter would automatically adjust the frequency. The operator would stop preloading when the counter indicates that the desired frequency, f', has been reached. The aforementioned necessity of counting nulls would be completely eliminated in such an instrument.

An important element of any ultrasonic technique for measuring bolt preloads is the transducer. Also of major importance is the method of applying the transducer to the bolt head in such a way that it does not interfere with normal wrench use. We have developed several schemes that satisfy these requirements. Although several attempts were made to incorporate transducers into socket wrenches, we have concluded that such an arrangement has many disadvantages. The top photograph of Figure 25 shows such a spring-loaded arrangement with the active transducer centered in the socket head. When the socket wrench is placed over the bolt head, the transducer is automatically positioned and pressed against the hex head surface. Coupling of ultrasonic energy into the bolt, of course, requires the use of grease or some other suitable couplant which can be applied to either the bolt or the transducer prior to placement of the wrench-probe assembly. This technique provides reasonably good echo patterns so long as the socket wrench is not moved. However, when the wrench is actually used to tighten the bolt, we find that the normal wrench wobble, which occurs during this operation, also affects the ultrasonic echoes. The observed changes were due to small, but undesirable, movement of the transducer. This problem was minimized by decreasing the mechanical coupling between the transducer and the wrench head, but completely satisfactory results were never really achieved using this type of arrangement.

The investigation of transducers led to two conclusions as follows: (1) Although there may be special applications where it will be useful to permanently incorporate a transducer into a wrench head, it appears much more reasonable to leave the transducer essentially independent of the wrench head, (2) Optimum results are obtained when the active transducer is damped with a suitable backing material.

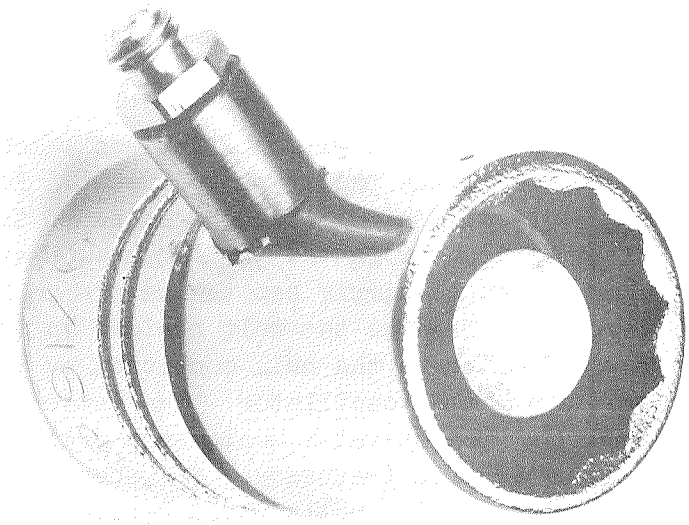

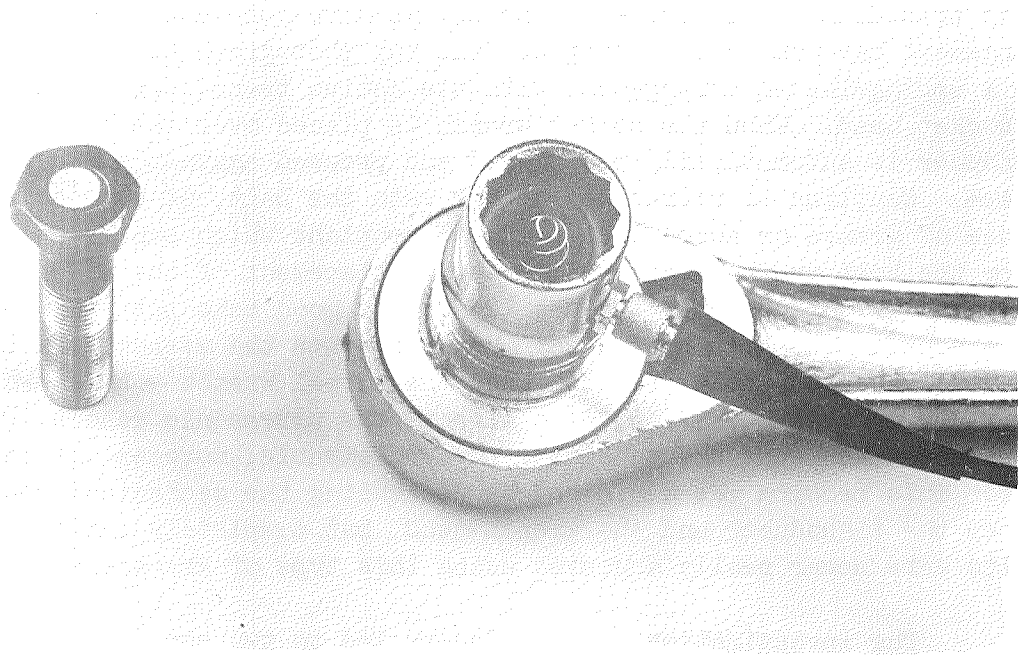

Figure 25 - Prototype Socket Wrench With Spring Loaded Transducer (Top) and Modified Socket Wrench With Electrical Contact for Separate Transducer (Bottom).

The conclusion regarding the transducer-wrench relationship is based on the wide variety of bolt head geometries and wrenching requirements. Even for one specific bolt configuration, space limitations associated with actual applications may necessitate the use of several different type wrenches. Thus if the transducers are incorporated into the wrench, a number of very specialized wrenches would be required for each bolt type. In contrast, if the transducer is independent of the wrench, then a single transducer may be used with a wide variety of bolt-wrench combinations. In this latter case only a simple modification of the wrench is required to provide electrical contact to the transducer.

One approach to the separate transducer idea is to simply use uncased piezoelectric elements. We have achieved good results with the LTZ-5 composition produced by Transducer Products of Torrington, Connecticut. This particular formulation has a somewhat lower capacitance than most other lead-titanate-zirconate materials, and thus does not have such a low impedance at high frequencies. The uncased transducer is greased onto the bolt head, then electrical connections are made with a modified wrench head (see Figure 25 - bottom). The bolt itself serves as the ground connection but it is usually desirable to insure this ground through the wrench housing and back to the electrical console. The second connection is made to the top electrode surface of the transducer by means of a light spring contact. With such arrangements the bolt can be completely tightened with no adverse effects due to transducer movement. If the wrench has to be removed during the torquing operation the electrical connections are broken, and the signal is lost. However, when the wrench is reapplied the signal returns and the ultrasonic measurement is made as if the connection had been continuous. Advantages of the uncased transducers include relatively low cost when purchased in quantity and relatively high signal levels when operated near resonance. Disadvantages include fragility, very small size, and relatively narrow bandwidth.

A second approach to the separate transducer technique, and the one we recommend, involves placing the active transducer element in a small button-type housing which greatly reduces fragility and handling problems. A small amount of backing material can also be included in the housing to provide additional damping to the transducer. The latter will generally reduce the available signal levels at resonance but it increases the bandwidth and thus facilitates use of a given transducer over a wider range of frequencies. The greater damping also facilitates use of shorter pulse durations which sometimes reduces confusion due to superposition of the desired echo and spurious signals. We have tried different materials for backing applications and have found several epoxy formulations that give good results. Metal powders have been mixed with some epoxies to give increased damping but clear epoxy is satisfactory. Figure 26 shows a cross sectional view of a small transducer housing.

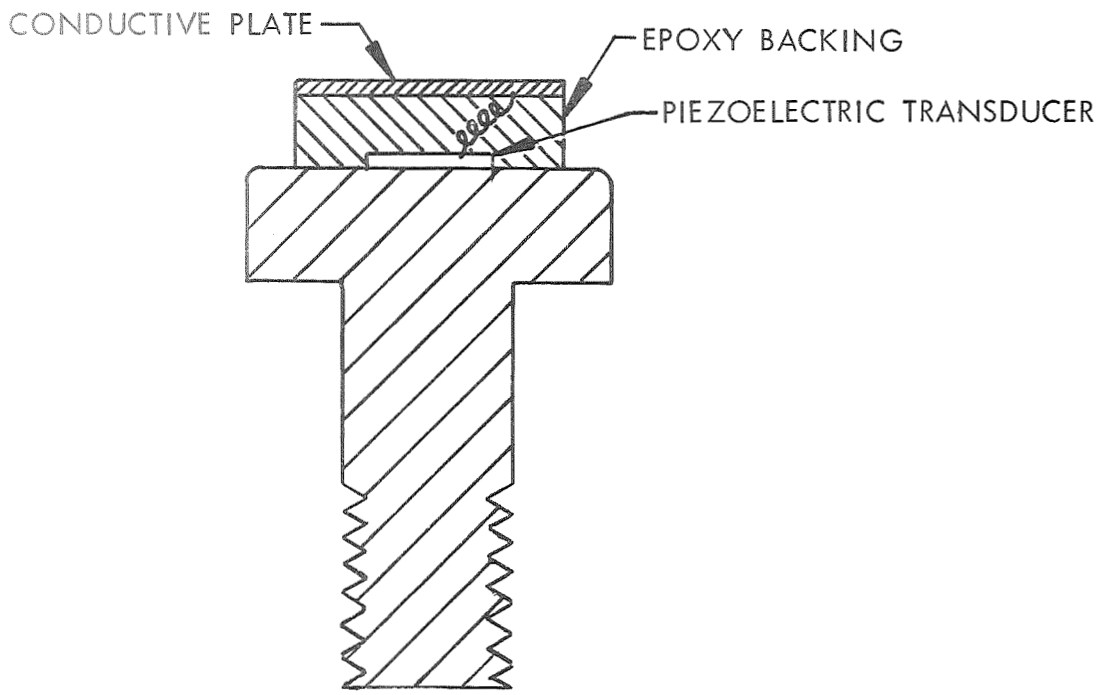

Figure 26 - Cross-Sectional View of Small Cylindrical Transducer Unit Mounted on Bolt Head. A small spring clip affixed to the wrench will make electrical contact with the conductive plate during torquing operations.

Several of the actual transducers, custom made for this program, are shown in Figure 27.

In applications involving flat hex head bolts it is desirable to use relatively short transducers because of their increased stability and resistance to tilting forces that might be exerted by the spring contact on the top surface. For bolts which have lightening holes in the head, it is necessary to use taller units, but the diameter of the housing can be designed to fit into the lightening hole in such a way that a little excess grease gives the transducer excellent stability. Illustrations of the above transducer applications and methods of making the electrical connections are shown in Figure 28.

VII. CALIBRATION RESULTS

After the prototype instrumentation was completely assembled, calibration data were collected for a large number of bolts supplied by the Marshall Space Flight Center. Most of the bolts enumerated in Table I were calibrated along with additional ones shown in Figure 29. All titanium bolts were calibrated in the "as received" condition except that the head was hand surfaced slightly with 400 grit paper to remove roughness associated with identification numbers. The 3/4 in. aluminum bolts were treated similarly. The heads of all other bolts were machined slightly to reduce roughness or to make a flat bottom in an otherwise taper bottom lightening hole.

For calibration purposes, each bolt was hydraulically loaded in a Skidmore-Wilhelm torque-tension tester to a stress of about 0.4 of the ultimate tensile strength. The load was recorded along with the necessary bolt dimensions and the ultrasonic parameters, f and Δf. In most cases each bolt was loaded several times and the transducer was removed and re-applied between loading cycles.

After all of the bolts were examined the Δf and load data were used to calculate the term $(\beta/2 - \alpha)$, previously shown in Expression (3) and derived in Appendix A. Expression (3) can be solved for $(\beta/2 - \alpha)$ to give

$$(\beta/2 - \alpha) \cong \left(\frac{\ell_t \Delta f}{Lf}\right) \Big/ \left(\frac{\ell_s}{A_s} + \frac{\ell_{s'}}{A_{s'}}\right) \tag{4}$$

(Recall that the β term controls the stress-induced change in velocity of the ultrasonic waves and α, the reciprocal of Young's modulus, controls the stress-induced elongation of the bolt. Both of these terms should be constant for a given material.)

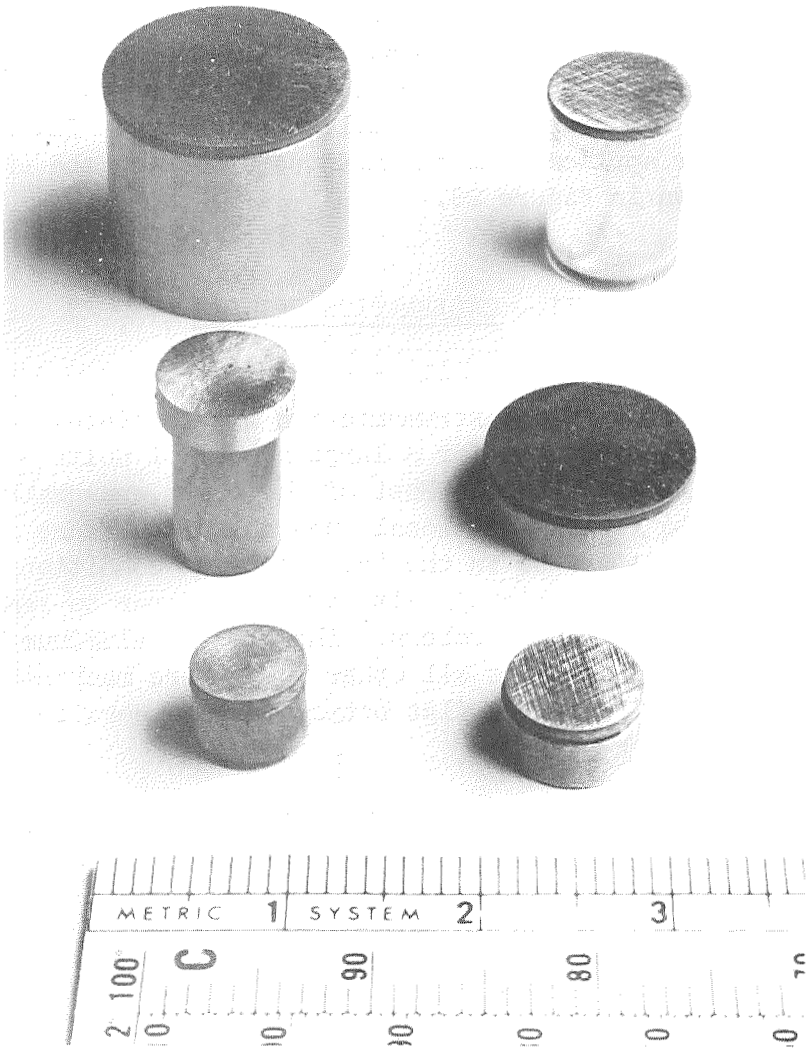

Figure 27 - Several Transducer Housings Designed for Specific Bolt Applications.

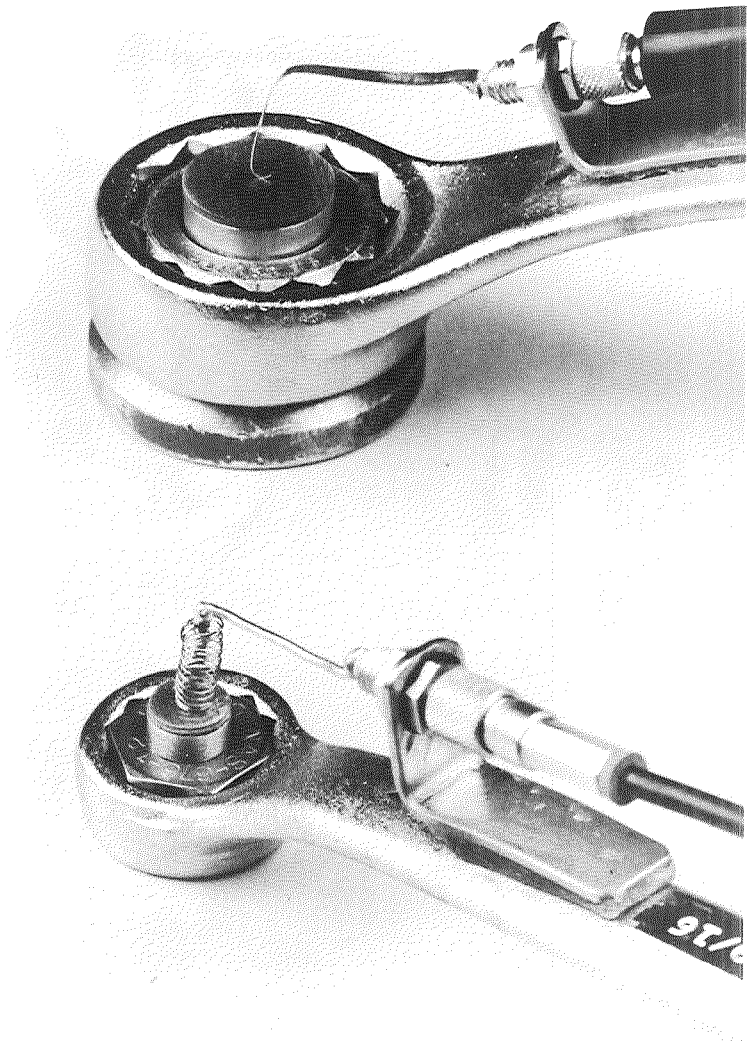

Figure 28 - Examples of Transducer and Wrench Connectors for Two Different Bolt Head Configurations. The top bolt has a lightening hole in the head whereas the bottom bolt has a flat hex head.

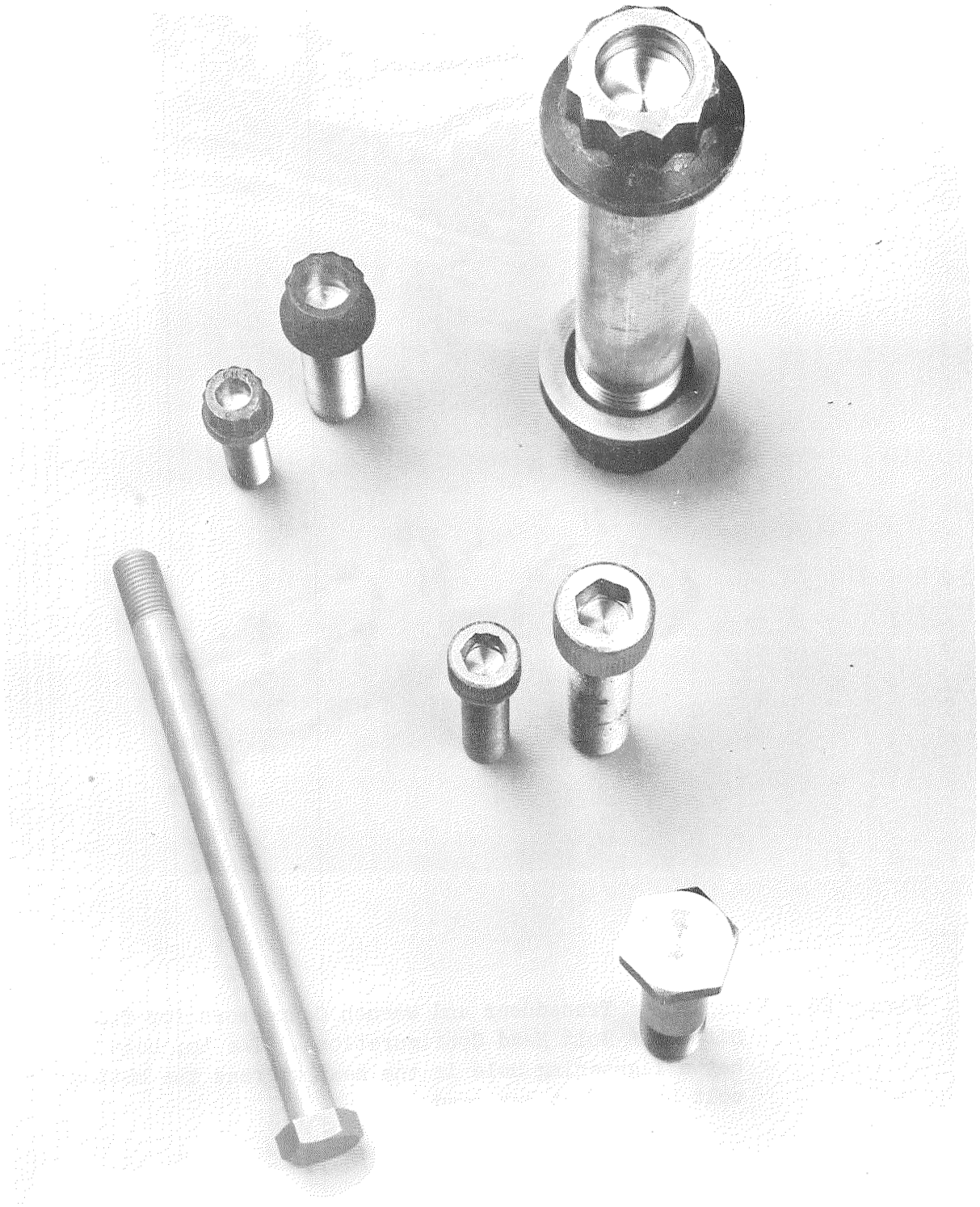

Figure 29 - Additional Bolts for Which Calibration Data Were Collected.

We would expect the value of $(\beta/2 - \alpha)$ for a given material to be constant regardless of the bolt size. However, it should be pointed out that third order elastic constants, which are included in the β term, do depend significantly on the alloy and on the grain orientation. Young's modulus sometimes also varies several percent between different alloy compositions. These variations have been tabulated by Smith et al.,[10] for a few materials.

In evaluating the term $(\beta/2 - \alpha)$, hereafter called K, we have defined the stressed lengths of the bolt as previously shown in Figure 4. This is an arbitrary definition for the stressed region does extend somewhat beyond these boundaries. Some stress analysts add to the above length an increment of length equal to three times the thread pitch. The definition of the stressed length will certainly affect the value of K, but most of the resultant errors will be cancelled out if the same definition is used both during calibration and testing.

Table II contains the K values as they were calculated from the calibration data. Values are given for each type and size of bolt. The standard deviations are also tabulated along with information about the number of bolts examined and the total number of readings. We would like to make several general observations about the results enumerated in Table II and then a few brief comments about each group of bolts (alloy type). First, note that the K values for most alloys vary somewhat for different size bolts. Only the two 4140 steel bolts (MS 20006-14 and MS 20012-32) exhibited almost identical K values. The cause of the variations observed for other alloys is not well defined but some of the variation may be due to real differences in elastic properties. Another factor may be an over-simplification of the stress conditions and resultant inaccuracies in Expression (3). If this were the major factor, we might expect to see a monotonic trend in the K values for increasing bolt size but such a trend is not evident. Finally, we note that aluminum has by far the largest K values and 431 stainless has the smallest. The remaining steels all exhibit K values that vary over a relatively small range.

TABLE II

SUMMARY OF CALIBRATION DATA

Material	Bolt Size	Identification	$\bar{K} \pm \sigma (in^2/lb)$	Number of Bolts	Number of Readings
A-286 Steel	7/8 in. - 14	RD 111-4009-4454	$-(1.53 \pm 0.01)10^{-7}$	3	13
AMS 5736 Steel	3/8 in. - 24	MS 9036-12	$-(1.38 \pm 0.03)10^{-7}$	3	13
	1/2 in. - 20	MS 9038-15	$-(1.47 \pm 0.18)10^{-7}$	3	8
4140 Steel	3/8 in. - 24	MS 20006-14	$-(1.36 \pm 0.02)10^{-7}$	2	8
	3/4 in. - 16	MS 20012-32	$-(1.38 \pm 0.03)10^{-7}$	2	6
Steel ?	1/4 in. - 28	NAS 1304-8W	$-(1.22 \pm 0.04)10^{-7}$	2	4
	3/8 in. - 24	NAS 1306-12W	$-(1.38 \pm 0.01)10^{-7}$	2	8
	3/4 in. - 16	NAS 1312-29	$-(1.17 \pm 0.05)10^{-7}$	2	10
Steel?	3/8 in. - 24	MS 16998-46	$-(1.63 \pm 0.09)10^{-7}$	3	11
(Cap Screws)	1/2 in. - 20	MS 16998-99	$-(1.32 \pm 0.08)10^{-7}$	2	5
431 Stainless	1/4 in. - 28	AN4C-10	$-(0.84 \pm 0.02)10^{-7}$	5	6
	3/8 in. - 24	AN6C-14	$-(1.10 \pm 0.02)10^{-7}$	1	2
	3/4 in. - 16	AN12C-36A	$-(1.05 \pm 0.06)10^{-7}$	2	4
Aluminum	1/4 in. - 28	AN4DD-10A	$-(4.24 \pm 0.01)10^{-7}$	2	3
	5/16 in. - 24	AN5DD-11A	$-(4.85 \pm 0.08)10^{-7}$	2	5
	3/8 in. - 24	AN6DD-47A	$-(4.05 \pm 0.03)10^{-7}$	3	6
	3/4 in. - 16	AN12DD-H35A	$-(4.62 \pm 0.02)10^{-7}$	2	3
Titanium					
All BM	1/4 in. - 28	NAS674V8	$-(2.25 \pm 0.08)10^{-7}$	3	3
All Camcar	1/4 in. - 28	NAS674V8	$-(1.57 \pm 0.04)10^{-7}$	2	2
1 BM-2 Camcar	3/8 in. - 24	NAS676V12	$-(1.48 \pm 0.04)10^{-7}$	3	3
All VB	1/2 in. - 20	NAS678V21	$-(1.64 \pm 0.04)10^{-7}$	3	7

The following specific comments are for the indicated alloy:

A286 Steel: Three large bolts of this high strength steel were examined and the results were remarkably reproducible. A plot of Δf-versus-load data gave a straight line with very little scatter.

AMS 5736 Steel: There is variation of about 6% between values for the 3/8 in. and 1/2 in. bolts. The much larger standard deviation observed in the data for the 1/2 in. bolts may be due to any number of factors where the sample number is so small. At any rate, a relatively small error would result if an intermediate value of K were used for both bolts.

4140 Steel: Little comment is required here. Excellent agreement was obtained between the different size bolts and the data scatter was small.

Tool Steel: Various size bolts exhibited K values which appear to be significantly different. The total variation amounts to about 18%.

Steel Cap Screws: The K values differ by about 20%. Incidentally, these caps screws and any other bolts which use internal wrenching probably present the greatest problem to successful ultrasonic analysis of preloads.

431 Stainless: This alloy gave some rather unusual results in that a number of the 3/8 in. and 3/4 in. bolts did not exhibit a completely linear relationship between Δf and load. Figure 30 shows the two distinctly different types of data obtained. Of the seven 3/4 in. bolts examined, only two exhibited response characteristics similar to that of Curve A, whereas five produced data like Curve B. For the latter five, the break in the slope occurred at about the same load and the Δf at maximum load was quite reproducible. There was no indication that these bolts were from different lots but the dissimilarities were striking. Table II contains only data for those bolts which did give a linear response over the whole range. We were never able to completely explain the nonlinear characteristics of the other stainless bolts, but we believe that they may be related to a combination of magnetic effects and residual stresses. 431 is ferromagnetic and as such it could exhibit a strong "ΔE" effect, i.e., a change in Young's modulus related to the degree of magnetization. Furthermore, the stable orientation of domains in a ferromagnetic material depends on crystal structure and stress. Thus, we have theorized that in those bolts which exhibited a break, a residual stress may have been present which produced a net domain alignment perpendicular to that caused by tensile stresses along the bolt axis. When the tensile stress effect became large enough to overcome the residual stress effect, the domains started to realign themselves, resulting in a slight change in Young's modulus and perhaps a break in the Δf data.

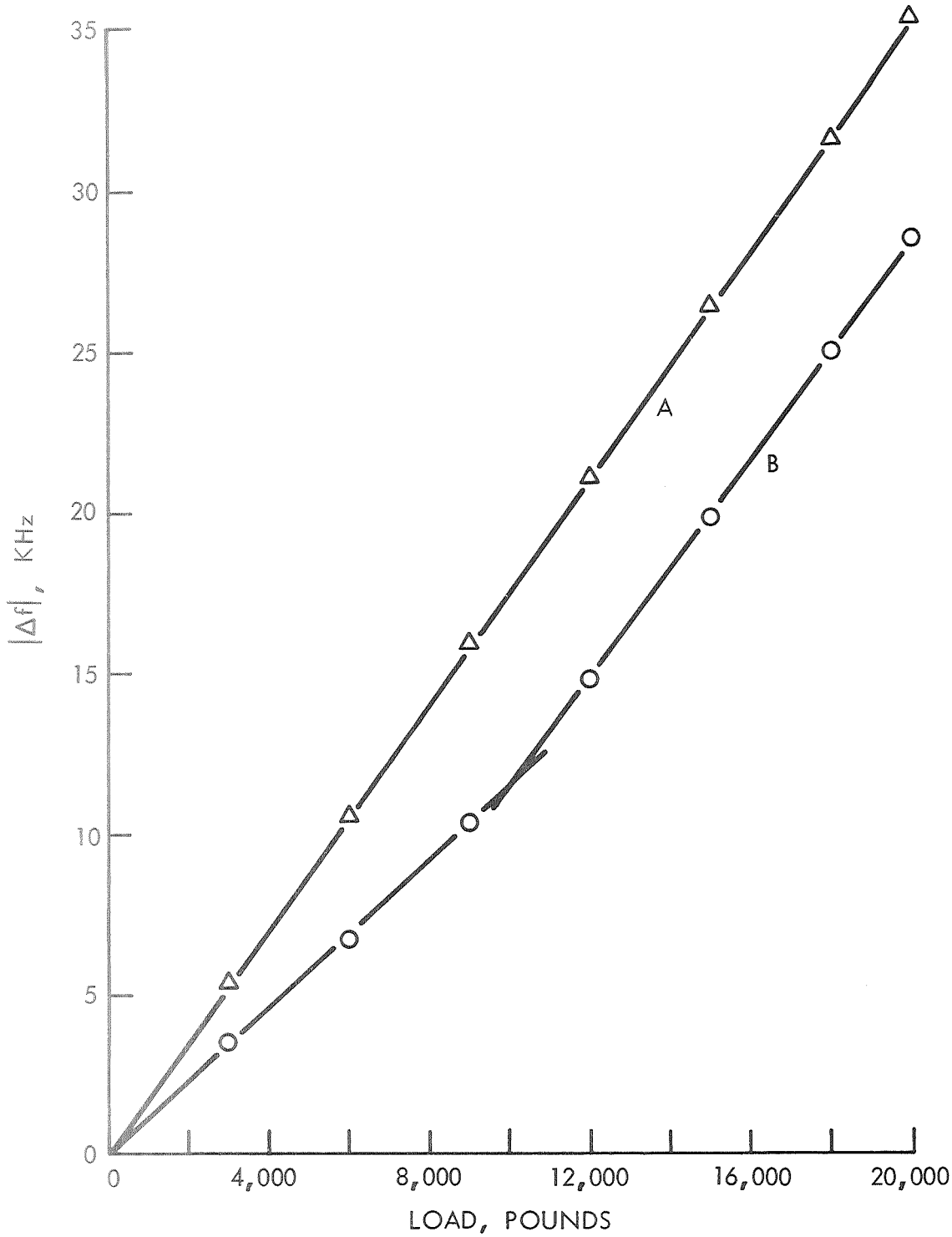

Figure 30 - Δf-Versus-Load for Two Different 3/4-In. Bolts of 431 Stainless Steel

We performed a few experiments with a magnetic field which did influence the Δf readings, but we were unable to definitely confirm the theory mentioned above. All of the 1/4 in. bolts examined exhibited the normal linear response without the break observed in the 3/8 in. and 3/4 in. bolts.

Aluminum: The specification covering the manufacture of these bolts permits the use of several alloys. This may explain some of the observed variations between different size bolts. As mentioned previously, aluminum undergoes a relatively large change in velocity and length for a given stress.

Titanium: Whereas the lot origin of most of the steel and aluminum bolts was impossible to identify, the titanium bolts were clearly marked as coming from three different suppliers. The three supplier marks were BM, Camcar, and VB. Furthermore, all bolt identification numbers contained a V which supposedly indicates that the alloy is 6% aluminum-4% vanadium. The specification covering the manufacture of these bolts permits use of either the 6Al-4V alloy or a 4Al-4Mn alloy. Of the five 1/4 in. bolts inspected, three were identified BM and two carried the Camcar mark. The two BM bolts had a much larger K value than the three Camcar bolts. Although all of these bolts contained a V in the identification number, some real differences exist in the physical properties. For example, we found that the Camcar bolts had a significantly greater hardness than the BM bolts. Of the three 3/8 in. titanium bolts one carried the BM mark and two bore the Camcar mark. All of the 3/8 in. bolts gave K values fairly close to the 1/4 in. Camcar bolts. Furthermore, we were unable to observe significant differences in hardness between the BM and Camcar bolts of the 3/8 in. size. All of the 1/2 in. bolts bore the VB mark.

The titanium data certainly suggest that, at least for that alloy, Δf results may vary significantly between bolts of a different lot. This variation may be due to different heat treatments or perhaps the use of an entirely different alloy. Further study of this problem is definitely needed prior to final acceptance of ultrasonic techniques for measuring preloads.

There is one additional observation that can be made regarding Table II and the K values determined from our ultrasonic measurements. Once again we recall that $K = (\beta/2 - \alpha)$, and that β controls the stress-induced elongation of the bolt. From our data we can evaluate β from knowledge of K and α. For all the bolts inspected during this program β has a negative value and the ultrasonic velocity decreases with increasing tensile stress. Thus, the velocity change increases the transit time just as the increased elongation does. The magnitude of $\beta/2$ is generally 2 to 3 times as large as α so the velocity effect is greater than the elongation effect.

Earlier in this section it was mentioned that β can be calculated directly from second and third order elastic constants. Smith et al.,[10] have tabulated these constants for several different materials. The alloys studied by Smith and those used in this program were not identical, but for comparison purposes we used some of his data to calculate β. Using an average K value for the steel bolts of -1.3×10^{-7} in^2/lb, we get $\beta = -1.94 \times 10^{-7}$ in^2/lb. From the Smith data for REX 535 steel we calculated a value of $\beta = -1.57 \times 10^{-7}$ in^2/lb. The only other material on which we could make a comparison is aluminum. From our data we used $K = -4.5 \times 10^{-7}$ in^2/lb as an average and thus obtained $\beta = -7.05 \times 10^{-7}$ in^2/lb. The Smith data for B53S-P (5554) aluminum yielded a β value of -6.89×10^{-7} in^2/lb. The agreement in these two cases is fairly good considering the fact that the alloys are not identical.

The K values presented in Table III can be used with Expression (3) to calculate the desired Δf for a wide range of bolt and load conditions. However, until additional experience is gained through use of the ultrasonic analyzer, it may be more practical to approach a few specific problems in the following way. First, simulate the bolt application in a torque-tension tester, i.e., duplicate the stress length and load conditions using bolts identical to those used in the actual application. Determine Δf for this specific load condition, then simply torque the bolts in the final application to this same frequency change.

VIII. RECHECK CAPABILITY

The major differences that exist between analyzing bolt loads during assembly and subsequent to assembly have been discussed previously, but some further comments regarding the recheck capability are in order. The preload determination requires only a short term measurement of relative change in the frequency of a given null. The recheck capability requires a comparison of two absolute transit time measurements which may be made weeks or months apart.

There are several ultrasonic techniques which can provide high accuracies in measuring absolute transit times, but there is more to the recheck problem than simply measuring the transit time. For example, consider the round trip transit times for two bolts which are identical in every respect except length. Let one bolt be 2.000 in. long and one 2.010 in. long. The fractional difference in transit time between these bolts is $0.01/2.0 \cong 0.005$. This value is of the same order of magnitude as the fractional change in transit time produced by stresses. Thus, it is quite obvious that if transit time measurements are to be of any value in rechecking bolt loads, at least one of the following conditions

must be met: (1) the total lengths and stressed lengths of bolts used in a specific application must have variations of less than about 0.001 in., or (2) record keeping will be necessary for comparative reading on each bolt. The second condition is probably the most acceptable solution.

A very limited investigation of the recheck problem was performed during this program. Absolute transit time measurements were made on a few bolts and a rough correlation with stress level was achieved. These measurements were made by scanning across a set number of nulls and then defining the parameter ΔF discussed in Section III.

The reproducibility of ΔF measurements generally increases as the number of nulls increases. Thus, once again it is desirable to use damped transducers with wide bandwidths. Further study of the recheck problem should be directed at establishing error limits for a very limited number of bolts under conditions of both permanently affixed and removable transducers. Careful consideration should also be given to the influence of temperature changes and methods of compensating for such changes.

IX. CONCLUSIONS AND RECOMMENDATIONS

The results achieved during this program clearly indicate that ultrasonic techniques can be quite useful in evaluating bolt preloads. Potential accuracies are much higher than those of torque wrenches or PLI-washers, but a number of factors can reduce practical accuracies below the inherent maximum. Although additional testing and evaluation are always desirable, we offer the following conclusions based on results to date.

1. Most bolts can be tested satisfactorily at a frequency of 7.5 to 8.0 MHz.

2. Simple hex head bolts can be inspected in the "as received" condition if there is an adequate flat area ($\sim$ 3/8 in. diameter) near the middle of the head with a surface finish of 100 μin. RMS or better. The opposing end (threaded end) can be somewhat rougher (200 μin. RMS) but it should be within about 1 degree of parallel to the head surface.

3. Bolts with recessed lightening holes in the head can be inspected also. The bottom of the lightening hole should meet the same conditions outlined above for hex head bolts.

4. Transducers are easily applied to the bolt head with a suitable couplant such as silicone vacuum grease. Electrical connections to the transducers can be made by spring clips attached to a wrench or

other torquing device. Some difficulty may be encountered in applying transducers and making satisfactory electrical connections on bolts with internal wrenching holes.

5. The inherent errors of the interferometric methods developed during this program are less than ± 1%. However, other factors including variations in material properties and dimensions may increase the errors to more than 10%. For critical applications, where fairly tight tolerances are held on dimensioning and material variability, errors of less than 2-3% are easily attainable.

6. Temperature variations produce no problems in measuring bolt preloads if, during assembly, the bolts are in approximate thermal equilibrium with their surroundings.

7. Bending effects can produce significant amounts of data scatter; however, the ultrasonic interferometer responds to these bending effects through much the same mechanism that it responds to pure tensile stresses. The resultant scatter is indicative of real variations in tensile stress conditions. The influence of bending is minimized by centering the transducer on the bolt axis.

8. In laboratory tests where ultrasonic measurements can be made concurrent with load measurements, the deviation of Δf-versus-load plots from linearity gives a very accurate indication of the onset of plastic yielding. Such tests may be useful in evaluating bolt performance or material variability.

9. Our calibration data suggest that increased accuracy will be achieved if separate calibrations are used for different size bolts even when all bolts are of the same material. The reason for this is still unknown.

10. Although this program did not emphasize development of a technique with capability for rechecking bolt loads subsequent to assembly, there is a possibility that the same instrumentation can be used for this purpose. Further work is required to establish the accuracy and reproducibility of such measurements.

Recommendations:

1. Prior to extensive use of the interferometer technique, we recommend that the following procedures be used for one or more specific bolt applications where high accuracy in preload analysis is desired. First, simulate the actual stress length and load conditions as close as possible in a torque-tension tester. Determine the Δf value corresponding

to the desired hydraulic load level for at least five bolts. Average the results and use this mean as the calibration value. Then torque 5-10 bolts to the above Δf value and read the load directly from the gage on the torque-tension tester. The spread in the latter readings should be representative of that experienced in the actual application.

2. In order to evaluate the relative accuracies and ultimate potential of ultrasonic techniques in measuring bolt preloads, we recommend that a comparison be made between the interferometer technique and the time-of-flight technique as both are applied to the same set of bolts. Such a comparison would facilitate the selection of the most adequate technique for a desired degree of accuracy.

3. Further studies should be directed toward the development of recheck capabilities based on comparative measurements of absolute transit times.

REFERENCES

1. Hughes, D. S. and J. L. Kelly, Phys. Rev., 92, 1145 (1953).

2. Bergman, R. and R. Shahbender, Jour. App. Phys., 29, 1736 (1958).

3. Benson, R. W. and V. J. Raelson, Product Engineering, 30, 56 (1959).

4. Waterman, P. C. and L. J. Teutonico, Jour. Appl. Phys., 28, 266 (1957).

5. McSkimin, H. J., Jour. Acoust. Soc. Amer., 37, 864 (1965).

6. Papadakis, E. P., Jour. Appl. Phys., 35, 1474 (1964).

7. Pervushin, I. I. and L. P. Filippov, Soviel Phys.-Acoustics, 7, 307 (1962).

8. Benson, R. W. and Associates, Inc., NASA Report No. N68-21875 (1968).

9. McFaul, H. J. and B. G. Martin, Douglas Aircraft Company Report No. MDC-J0913/01, dated 10/6/70.

10. Smith, R. T., R. Stern, and R. W. B. Stephens, Jour. Acoust. Soc., 40, 1002 (1966).

APPENDIX A

FREQUENCY-NULL RESPONSE FOR STRESSED BOLTS

Consider the bolt sketch previously shown in Figure 4a where the overall bolt length is ℓ_t . Prior to stress application, the ultrasonic path length would be $2\ell_t$. Assume that the ultrasonic frequency is adjusted for a null condition which should occur approximately when an integral number, N , wavelengths fit into the total path length. Thus,

$$N = 2\ell_t f_o/v_o \quad . \tag{A-1}$$

There are other factors such as phase changes at the transducer and bolt end which will alter Expression (A-1) but as long as these factors remain constant, the end results of the following derivation will not be affected.

Now assume that the same null is maintained by changing the frequency to f' as a tensile load is applied to the bolt. The tensile load is, of course, only applied over the length ℓ_s , but it produces a change, $\Delta\ell$, in the overall length and a new velocity v' in the stressed region. We can now write

$$N = 2\left[\frac{\ell_t-\ell_s}{v_o} + \frac{\ell_s+\Delta\ell}{v'}\right] f' \quad . \tag{A-2}$$

But since the same null condition is maintained, the integer N is the same in (A-1) and (A-2). These expressions can then be equated and we obtain

$$\ell_t f_o/v_o = \left(\frac{\ell_t-\ell_s}{v_o} + \frac{\ell_s+\Delta\ell}{v'}\right) f' \tag{A-3}$$

which can be simplified to

$$\frac{\Delta f}{f'} = \frac{\ell_s}{\ell_o}\left[1 - \frac{v_o}{v'}\left(1 + \frac{\Delta\ell}{\ell_s}\right)\right] , \tag{A-4}$$

where $\Delta f = f'-f_o$. However, the term $\Delta\ell/\ell_s$ is equal to the elastic strain, $\epsilon = S/E$, where S is the stress and E is Young's modulus. We can also write $v' = v_o(1+\beta S)^{1/2}$ where $\beta = \gamma/\rho v_o^2$ and γ is a constant

for a given material and ρ is the density. For a better understanding of the significance of γ, the reader is referred to the following reference (R. T. Smith, Ultrasonics, 1, 135, 1963). Expression (A-4) can then be written as

$$\frac{\Delta f}{f'} = \frac{\ell_s}{\ell_t} \left[1 - \frac{v_o(1+\alpha S)}{v_o(1+\beta S)^{1/2}} \right] \qquad \text{(A-5)}$$

where $\alpha = 1/E$. Since $\alpha S \ll 1$ and $\beta S \ll 1$, we can approximate expression (A-5) as follows:

$$\frac{\Delta f}{f'} \cong \frac{\ell_s}{\ell_t} (\beta/2 - \alpha) S \quad . \qquad \text{(A-6)}$$

Thus, we see that $\Delta f/f'$ is linear with stress, S, and depends on the dimensions ℓ_s and ℓ_t, as well as the material constants, β and α.

For bolts having two different cross-sectional areas within the length ℓ_s (see Figure 4b), it is necessary to write

$$\frac{\Delta f}{f'} \cong \frac{(\beta/2 - \alpha)}{\ell_t} (S\ell_s + S'\ell_{s'}) \qquad \text{(A-7)}$$

where S is the stress in length ℓ_s and S' is the stress in length $\ell_{s'}$. Since the stress in each sublength is related to the overall load, L, and the effective cross-sectional area, A, we can alternatively write (A-7) as follows:

$$\frac{\Delta f}{f'} \cong \frac{(\beta/2 - \alpha)}{\ell_t} \left(\frac{\ell_s}{A_s} + \frac{\ell_{s'}}{A_{s'}} \right) L \quad . \qquad \text{(A-8)}$$

In expressions (A-6) through (A-8) the original frequency f_o could be substituted for f' with little loss in accuracy since they differ by less than one part in 100.

MSFC—RSA, Ala